



1 **REVIEW: The Greater Agulhas Current System – Circulation, Variability, 2 Long-Term Trends and Impacts on Weather, Climate and Ecosystems**

3

4 Issufo Halo^{1,2}, Tarron Lamont^{1,2,3,5}, Michael G. Hart-Davis^{2,6}, Pierrick Penven⁴, Isabelle
5 Ansorge⁵, Chris Reason⁵, Björn Backeberg^{2,7,16}, Siren Rühs^{9,10}, Erik van Sebille¹¹, Christo
6 Whittle^{2,12}, Annette Samuelsen^{2,7}, Johnny Johannessen^{2,7,8}, Tamaryn Morris¹³, Marjolaine
7 Krug^{1,2}, Juliet Hermes^{5,13}, Marek Ostrowski^{2,15}, Sheveenah Taukoo^{2,5}, Babatunde J. Abiodun^{2,14}

8

9 ¹Oceans & Coasts, Department of Forestry, Fisheries and the Environment, Cape Town, South Africa

10 ²Nansen-Tutu Center for Marine Environmental Research, Oceanography Department, University of Cape Town,
11 Cape Town, South Africa

12 ³Bayworld Centre for Research and Education, Cape Town, South Africa

13 ⁴Laboratoire d’Oceanographie Physique et Spatiale (LOPS), University of Brest, CNRS, Ifremer, IRD, IUEM,
14 Plouzane, France

15 ⁵Department of Oceanography, University of Cape Town, Cape Town, South Africa

16 ⁶Deutsches Geodätisches Forschungsinstitut, Technische Universität München, Bayern, Germany

17 ⁷Nansen Environmental and Remote Sensing Center, Bergen, Norway

18 ⁸Geophysical Institute, University of Bergen, Bergen, Norway

19 ⁹GEOMAR Helmholtz Centre for Ocean Research Kiel, Kiel, Germany

20 ¹⁰Christian-Albrechts-Universität zu Kiel, Kiel, Germany

21 ¹¹Institute for Marine and Atmospheric Research, Utrecht University, Utrecht, Netherlands

22 ¹²Council for Scientific and Industrial Research (CSIR), Natural Resources and the Environment, Cape Town,
23 South Africa

24 ¹³South African Environmental Observation Network, Egagasini Node, Cape Town, South Africa

25 ¹⁴Climate System Analysis Group, Department of Environmental and Geographical Science, University of Cape
26 Town, Cape Town, South Africa

27 ¹⁵Institute for Marine Research, Bergen, Norway

28 ¹⁶Deltares, Delft, The Netherlands

29

30 *Correspondence:* Issufo Halo (ihalo@dfpe.gov.za)

31

32 **Abstract.** The Greater Agulhas Current System (GACS) is a dynamically complex western
33 boundary current system that plays a central role in inter-ocean exchange between the Indian and
34 Atlantic Oceans, regional weather and climate over southern Africa, and marine ecosystem
35 variability along the southeast African margin. Since the publication of The Agulhas Current
36 Book nearly two decades ago, major advances in ocean observing systems, satellite remote
37 sensing, numerical modelling, and interdisciplinary research have substantially expanded
38 understanding of the system. Here we provide an integrated review of progress over the period
39 2006–2025, synthesising recent advances across all components of the GACS, from its upstream
40 source regions to its downstream outflows and global climate connections. We first summarise
41 key technological and methodological developments that have transformed observation and
42 simulation of the Agulhas system, including sustained moored arrays, autonomous platforms,
43 multi-sensor satellite products, and high-resolution numerical models capable of resolving
44 mesoscale and submesoscale dynamics. We then reassess the state of knowledge for each sub-
45 region of the system: the East Madagascar Current, the Mozambique Channel, the Northern and
46 Southern Agulhas Current, the Agulhas Retroflection and leakage, and the Agulhas Return
47 Current, highlighting how recent studies have addressed uncertainties in circulation pathways,
48 variability, and connectivity. Knowledge developments include improved quantification of
49 transport variability and eddy dynamics in upstream source regions, new observational evidence
50 for eddy dissipation and momentum transfer within the Agulhas Current, refined understanding
51 of the processes governing retroflection and leakage, and growing insight into the role of
52 mesoscale and submesoscale dynamics in air–sea interaction, biogeochemical fluxes, and
53 ecosystem responses. We also review emerging evidence linking Agulhas system variability to



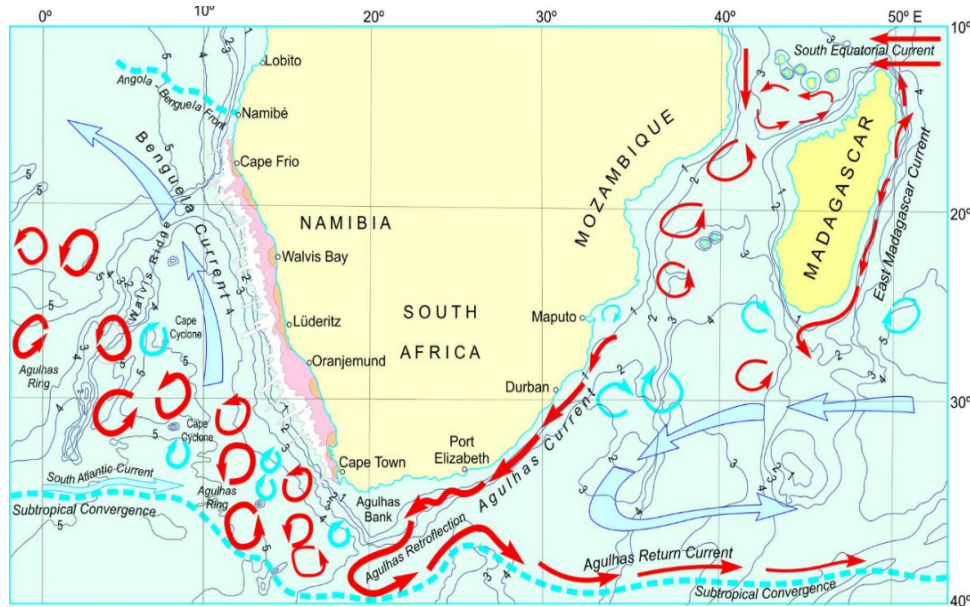
54 Southern Hemisphere wind forcing and to downstream impacts on the Atlantic Meridional
55 Overturning Circulation. We conclude by identifying remaining knowledge gaps and outlining
56 priority directions for future research, emphasising the importance of sustained observations,
57 improved representation of fine-scale processes in models, and stronger integration across
58 physical, biogeochemical, and ecosystem perspectives.

59

60 1. Introduction

61 The Greater Agulhas Current System (GACS; Fig. 1) is the western boundary current system of
62 the southwestern Indian Ocean, centred on the Agulhas Current (AC), which is considered to be
63 the strongest western boundary current in the Southern Hemisphere, and is embedded within the
64 wind-driven South Indian subtropical gyre (e.g., Beal et al., 2011; Lutjeharms, 2006). The system
65 comprises the source regions in the Mozambique Channel and along east Madagascar (including
66 the East Madagascar Current and associated undercurrent), the Agulhas Current proper along the
67 southeast African margin, the Agulhas Retroflexion at the southern tip of Africa, the eastward
68 Agulhas Return Current, and the intermittent Agulhas leakage of warm, saline Indian Ocean
69 waters into the South Atlantic via rings and filaments (e.g., Lutjeharms, 2006; Gordon, 1986).
70 These components are dynamically linked by mesoscale and submesoscale variability, including
71 eddies, meanders, filaments, and shelf–slope interactions, that collectively regulate the transport
72 of heat, salt, and other properties between the Indian, Atlantic, and Southern Oceans and mediate
73 downstream impacts on regional weather and ecosystems (e.g., Casal et al., 2009; Reason, 2001).

74



75

76 **Figure 1.** Schematic of surface ocean currents around southern Africa, covering the Benguela
77 and Agulhas Large Marine Ecosystem regions along the southwest and southeast African coasts,
78 respectively. Red (blue) colours denote warm (cold) currents. Background contours indicate
79 bathymetry, shown in kilometres. Adapted from Lutjeharms et al. (2007).

80 The volume transport of the Greater Agulhas Current System is dominated by the Agulhas
81 Current. Hydrographic and direct velocity measurements indicate that the Agulhas Current
82 carries a mean transport of approximately 84 Sv at the latitude of the South African east coast,
83 making it one of the strongest western boundary currents globally (Donohue et al., 2000; Beal



84 et al., 2015). The AC receives most of its waters from two main sources: the Mozambique
85 Channel and the Southern Madagascar region, which are fed primarily by the South Equatorial
86 Current (SEC) that transports an estimated 50–55 Sv between 10–16°S, upstream of the
87 Mascarene Plateau near ~60°E (New et al., 2007; Chapman, 2003; Lutjeharms, 2006). Along the
88 east coast of South Africa the AC flows southwestward with peak velocities exceeding 2 m s⁻¹
89 most of the time, and in situ measurements across the current indicate an estimated volume
90 transport of ~84 Sv (Donohue et al., 2000; Beal et al., 2015; Lutjeharms, 2006). At the southern
91 tip of Africa, the AC retroflects back into the Indian Ocean, shedding Agulhas rings which,
92 together with filaments and other (sub)mesoscale features, carry warm and saline Indian Ocean
93 waters into the southeast Atlantic, the Agulhas leakage, while the remaining flow turns eastward
94 as the Agulhas Return Current (ARC) (Gordon, 1986; Lutjeharms, 2006). Lagrangian estimates
95 further suggest that a non-trivial fraction of the AC transport contributes to leakage in the upper
96 1000–2000 m on the order of ~15–21 Sv, with the residual returning to the Indian Ocean via the
97 retroflection and ARC; the relative share varies on sub-seasonal to decadal time scales under the
98 combined influence of basin-scale wind forcing and mesoscale variability (Richardson, 2007;
99 Daher et al., 2020; Casal et al., 2009; Beal et al., 2015).
100

101 The Indian–Atlantic inter-ocean exchange associated with the Agulhas system modifies the
102 buoyancy structure of currents in the South Atlantic and has the potential to influence the strength
103 and stability of the Atlantic Meridional Overturning Circulation (AMOC), with implications for
104 global climate (Beal et al., 2011; Rühs et al., 2022; Schulzki et al., 2024). In particular, Agulhas
105 leakage, defined as the westward export of warm, saline Indian Ocean waters via rings, filaments,
106 and other (sub)mesoscale features, can increase the salt content of the upper limb of the AMOC
107 and thereby partly offset freshening tendencies in deep water formation regions (Gordon, 1986;
108 Beal et al., 2011). Over the past decades, modelling and observational studies have linked
109 variability and trends in leakage to Southern Hemisphere wind forcing and to large-scale
110 adjustments involving the Antarctic Circumpolar Current, highlighting that the magnitude and
111 timing of leakage are critical for communicating density anomalies into the Atlantic on
112 interannual to decadal time scales (Casal et al., 2009; Loveday et al., 2014; Durgadoo et al., 2013;
113 Rühs et al., 2022). At regional to local scales, the Agulhas Current's intense latent heat fluxes
114 and mesoscale variability also shape the weather and climate of southern Africa, providing
115 moisture and instability to systems that produce heavy rainfall along the east and south coasts
116 (Reason, 2001), thereby underscoring the dual role of the GACS as both a regulator of global
117 overturning and a driver of regional climate impacts.
118

119 Beyond its role in large-scale circulation and climate, the dynamics of the Agulhas Current
120 System exert a strong control on regional and local ocean biogeochemistry along the southeast
121 African margin. The intense mesoscale and submesoscale variability of the system, including
122 eddies, meanders, filaments, and shelf-slope interactions, modulates vertical and lateral
123 exchanges of nutrients, oxygen, and carbon between the open ocean and the continental shelf,
124 thereby shaping patterns of biological productivity and ecosystem functioning
125 (Lutjeharms, 2006; Jackson et al., 2012; Jacobs et al., 2022). Interactions between the Agulhas
126 Current and the shelf promote episodic upwelling, cross-frontal exchange, and offshore
127 advection of shelf waters, influencing nutrient supply to the euphotic zone and driving spatially
128 heterogeneous primary production along the coast and over the Agulhas Bank (Lutjeharms
129 et al., 2000; Jackson et al., 2012). In the source regions of the current, particularly the
130 Mozambique Channel and south of Madagascar, mesoscale eddies have been shown to structure
131 nutrient distributions and biological responses across multiple trophic levels, linking physical
132 variability to ecosystem dynamics (Lutjeharms, 2006; Barlow et al., 2014). Through these

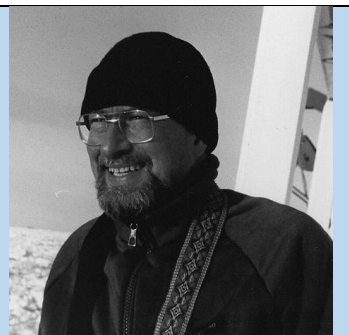


133 processes, the Agulhas system acts not only as a conduit for water-mass exchange, but also as a
134 regulator of biogeochemical fluxes and marine ecosystem variability at regional to local scales.
135

136 Because of its demonstrated importance for global ocean circulation and climate, its influence
137 on regional weather and climate over southern Africa, and its central role in shaping regional and
138 local ocean biogeochemistry and ecosystems, the Agulhas Current System has been the focus of
139 extensive scientific investigation at both regional and international levels. Sustained
140 observational programmes, targeted process studies, and numerical modelling efforts have
141 sought to improve understanding of the structure, variability, and impacts of the system across a
142 wide range of spatial and temporal scales (Lutjeharms, 2006; Beal et al., 2011; Biastoch
143 et al., 2024). This research has been driven by long-standing questions concerning the sources
144 and variability of the Agulhas Current, the mechanisms governing its retroflection and leakage,
145 and the implications of inter-ocean exchange for the Atlantic Meridional Overturning Circulation
146 and global climate, as well as by growing recognition of the system's role in modulating shelf
147 processes, marine productivity, and ecosystem responses along the southern African margin
148 (Reason, 2001; Jackson et al., 2012; Jacobs et al., 2022).

149
150 Following this sustained research effort, several syntheses and reviews of the Agulhas Current
151 System have been produced, reflecting its scientific importance and complexity (e.g. Beal et al.,
152 2011; Phillips et al., 2021; Biastoch et al., 2024). Most notably, the book *The Agulhas Current*
153 by Lutjeharms (2006) provided a comprehensive synthesis of several decades of observational,
154 theoretical, and modelling studies, and has since served as the primary reference describing the
155 physical oceanography and key processes of the Greater Agulhas Current System. This seminal
156 work consolidated knowledge of the current's source regions, structure, variability, retroflection
157 behaviour, and inter-ocean exchange, and identified a number of critical gaps in understanding
158 that required further investigation. Since the publication of this book nearly two decades ago,
159 however, substantial advances in ocean observing systems, satellite remote sensing, numerical
160 modelling, and interdisciplinary research have led to a rapid expansion of knowledge across all
161 components of the Agulhas system. These developments, together with the large and increasingly
162 dispersed body of literature produced since 2006, motivate the need for a new, integrated review
163 that reassesses the state of knowledge, synthesises recent insights, and identifies remaining
164 challenges and future research directions.
165

Professor Johann R. E. Lutjeharms (1944–2011) was one of the most influential physical oceanographers to emerge from southern Africa and a leading authority on the Agulhas Current system. Through pioneering observational, theoretical, and satellite-based studies, he fundamentally advanced understanding of western boundary currents, mesoscale variability, and inter-ocean exchange between the Indian and Atlantic Oceans. His work established the Agulhas system as a key component of the global overturning circulation and its role in climate variability. Beyond his scientific contributions, Lutjeharms played a defining role in building oceanographic capacity in South Africa through mentorship, institution-building, and international collaboration. His landmark monograph *The Agulhas Current* remains a foundational reference for researchers worldwide. His legacy endures through the scientific frameworks he established and the generations of oceanographers he trained.





167 This review is structured as follows. Section 2 provides an overview of the major technological
168 advances over the past two decades that have enabled new insights into the Greater Agulhas
169 Current System, including developments in in situ observing platforms, satellite remote sensing
170 capabilities, and numerical modelling frameworks. Section 3 synthesises the resulting progress
171 in scientific understanding across the principal components of the system. For each region, the
172 state of knowledge prior to 2006 is briefly summarised, followed by a review of key advances
173 derived from observational, modelling, and ecosystem-based studies. These sections address the
174 East Madagascar Current and its extensions, the Mozambique Channel, the northern and southern
175 Agulhas Current, the Agulhas Retroflection and leakage, and the role of the system in the global
176 climate circulation. Section 4 concludes the review by summarising the major findings,
177 highlighting remaining knowledge gaps, and proposing priority directions for future research
178 aimed at advancing understanding of this dynamically complex and globally significant current
179 system.
180

181 **2. Observational and modelling advances over the past two decades**

182 Over the past two decades (2006–2025), the capacity and capability to observe and model the
183 Greater Agulhas Current System (GACS) have expanded substantially, leading to significant
184 advances in understanding its circulation, variability, and impacts. This progress has been driven
185 by sustained developments in global and regional ocean observing systems, including the
186 expansion of in situ measurement networks, the emergence of autonomous observing platforms,
187 and improvements in satellite remote sensing coverage and resolution (Beal et al., 2011; Morris
188 et al., 2017; GOOS, 2025). In parallel, advances in numerical modelling, together with improved
189 atmospheric and oceanic reanalysis products, have enabled increasingly realistic simulations of
190 the GACS across a wide range of spatial and temporal scales (Beal et al., 2011; Biastoch et al.,
191 2024). These technological developments have played a central role in addressing many of the
192 knowledge gaps identified by Lutjeharms (2006) (see Section 3) and have underpinned much of
193 the scientific progress reviewed in this paper. The following subsections provide a high-level
194 overview of major advancements in in situ observing systems, satellite remote sensing, and
195 numerical modelling that have supported recent advances in Agulhas Current research.
196

197 The present-day state of the in situ and satellite-based observing is summarise in Fig. 2, and
198 described in more detail in Sect 2.1 and 2.2.
199

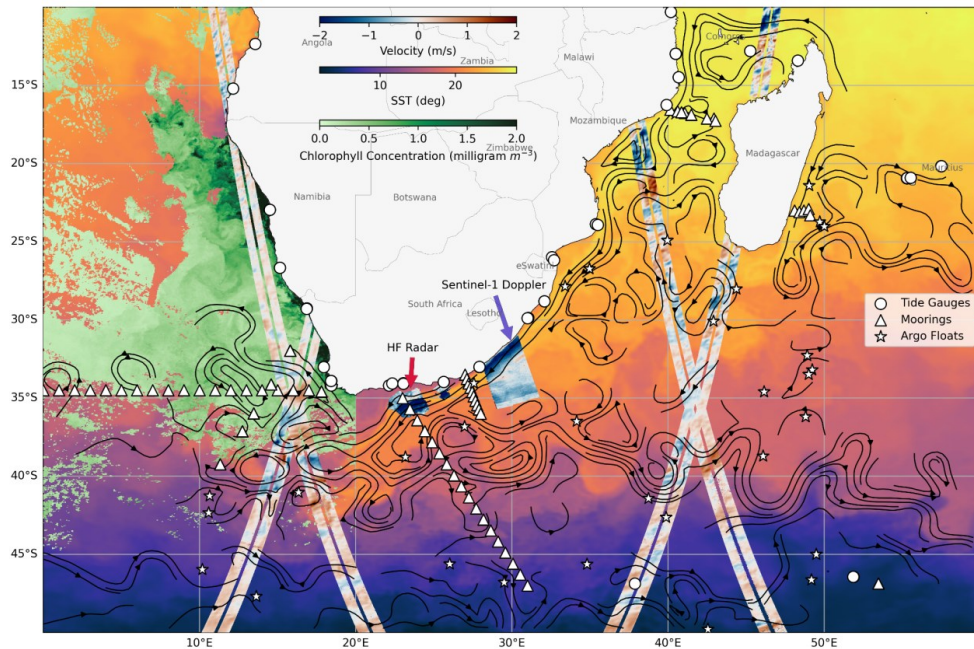


Figure 2. Observing system of the Greater Agulhas Current System. Circles indicate publicly available tide-gauge stations from the GESLA-4 dataset, triangles denote frequent mooring array locations, and stars show a snapshot of Argo float positions. Background shading represents satellite-derived sea surface temperature from the GHRSST product, while surface chlorophyll-a concentrations are obtained from GlobColour. Wide-swath geostrophic surface currents are shown from SWOT. Additional surface velocity measurements are provided by a daily snapshot from HF radar observations and Sentinel-1 Doppler-derived currents. Streamlines represent monthly mean geostrophic currents derived from satellite altimetry using the GlobCurrent product for June 2023.

2.1. Major advancements of in situ observing systems

Since 2006, in situ observing of the Greater Agulhas Current System has advanced substantially through the deployment of long-term moored arrays, repeated hydrographic sections, and the increasing use of autonomous platforms in both the source regions and along the Agulhas Current pathway.

Sustained mooring programmes in strategically important regions—including the Mozambique Channel, south of Madagascar, along the southeast African margin, and in the Cape Basin—have provided continuous, high-frequency time series of velocity, temperature, and salinity, enabling more robust estimates of volume transport and variability on seasonal to decadal time scales (Ullgren et al., 2012; Beal et al., 2015; Eliot and Beal, 2015; McMonigal et al., 2020). In the Mozambique Channel, the Long-term Ocean Climate Observation (LOCO) array delivered a decade-long record of the highly variable flow through the channel, while south of Madagascar the INdian–ATlantic Exchange (INATEX) moorings resolved the vertical structure and transport variability of the East Madagascar Current and its undercurrent (Ullgren et al., 2012; Ponsoni et al., 2015; Ponsoni et al., 2016). Along the Agulhas Current itself, large-scale mooring arrays deployed as part of the Agulhas Current Time-series (ACT) and Agulhas System Climate Array (ASCA) projects yielded new insights into the current’s volume transport and variability, while



228 downstream observations from the South Atlantic Meridional Overturning Circulation Basin-
229 wide Array (SAMBA) have supported quantification of interannual to decadal variability in
230 Agulhas leakage (Beal et al., 2015; Elipot and Beal, 2015; McMonigal et al., 2020). These
231 sustained moored observations have been complemented by dedicated ship based surveys and
232 repeat hydrographic transects, which have improved understanding of the vertical structure of
233 currents and water masses and provided essential context for interpreting the variability captured
234 by moorings (Ponsoni et al., 2015; Ponsoni et al., 2016; Hutchinson et al., 2013).

235

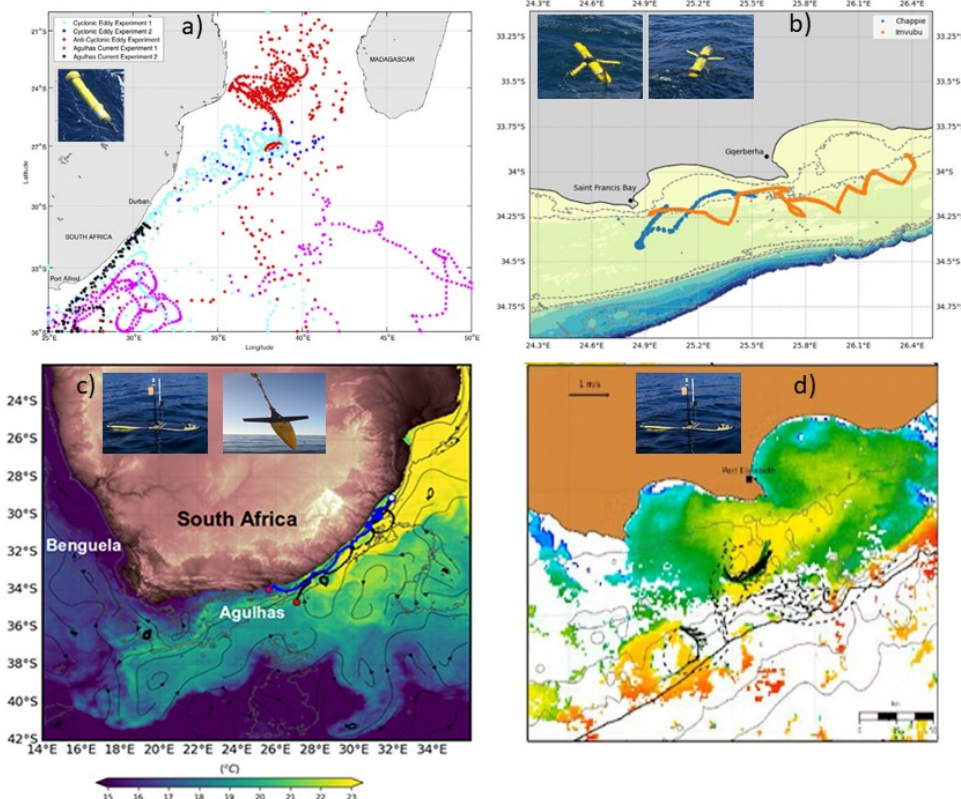
236 Ship based oceanographic surveys have remained a critical component of in situ observing of
237 the Greater Agulhas Current System by providing spatially extensive snapshots of physical,
238 chemical, and biological properties that complement sustained moored observations.
239 Coordinated regional programmes, most notably the Agulhas and Somali Current Large Marine
240 Ecosystems (ASCLME) project, enabled repeated multidisciplinary surveys across the
241 Mozambique Channel, around Madagascar, and along the southeast African margin,
242 significantly expanding hydrographic and ecosystem observations in the source regions of the
243 Agulhas Current (Vouzden et al., 2012; Halo et al., 2017). Long-standing survey efforts
244 conducted by the RV *Dr Fridtjof Nansen* under the EAF-Nansen Programme have provided
245 dense coverage of hydrographic stations in the western Indian Ocean, particularly in the
246 Mozambique Channel and around Madagascar, supporting investigations of circulation patterns,
247 water-mass properties, and ecosystem variability (Halo et al., 2017). Additional dedicated
248 surveys, including those associated with the INATEX programme and later IIOE-2 and
249 MADRidge initiatives, have resolved the vertical structure and variability of the East
250 Madagascar Current and its retroreflective behaviour, while repeat hydrographic transects such as
251 GoodHope and Crossroads have provided sustained measurements of physical, biogeochemical,
252 and biological properties across the Agulhas Current and Agulhas Return Current systems
253 (Ponsoni et al., 2015; Ponsoni et al., 2016; Hutchinson et al., 2013; Roberts and Ternon, 2020).
254 Many of these ship based surveys and autonomous deployments were multidisciplinary in nature,
255 integrating physical measurements with biogeochemical and biological sampling, thereby
256 enabling investigation of nutrient distributions, primary productivity, and ecosystem responses
257 alongside circulation variability (Vouzden et al., 2012; Barlow et al., 2014; Jackson et al., 2012;
258 Bezuidt and Makhala, 2024).

259

260 Autonomous observing platforms (Fig. 3) have increasingly complemented ship based surveys
261 and moored arrays by extending spatial and temporal coverage in regions where sustained
262 measurements are logistically challenging. Profiling Argo floats have contributed substantially
263 to observations of the Greater Agulhas Current System, and targeted deployments using high-
264 frequency sampling strategies have proven particularly effective in resolving mesoscale
265 variability in energetic regions such as the Mozambique Channel, south of Madagascar, and
266 along the Agulhas Current pathway (Morris and Lamont, 2019). These specialised deployments
267 enabled new in situ observations of eddy structure, propagation, and associated volume, heat,
268 and salt fluxes, including the first direct estimates of mesoscale eddy contributions to the Agulhas
269 Current derived from autonomous platforms (Morris et al., 2019). Buoyancy-driven ocean
270 gliders have further advanced understanding of fine-scale and submesoscale processes,
271 particularly along the inshore edge of the Agulhas Current, where early deployments revealed
272 the pervasive presence of shear-generated submesoscale cyclonic eddies (Krug et al., 2017).
273 Subsequent glider experiments, including GINA and later deployments along the southeast
274 African shelf, have provided high-resolution observations of frontal structure, turbulence, and
275 shelf-slope exchange processes that are not readily captured by conventional observing systems
276 (Krug et al., 2018; Pringle et al., 2022; d'Hotman et al., 2025). More recently, surface
277 autonomous vehicles, such as wavegliders, saildrones and sailbuoys, have been identified as a



278 promising addition to the in situ observing system, with the potential to provide sustained near-
279 surface and air-sea interaction measurements in energetic regions such as the Agulhas Current.
280



281
282 **Figure 3.** Collage of high-resolution in situ observational efforts in the Greater Agulhas Current
283 System over the past two decades. Panel (a) shows trajectories of 18 high-resolution Argo
284 profiling floats deployed between 2013 and 2017 in the southern Mozambique Channel and
285 along the southeast coast of South Africa (Morris and Lamont, 2019). Panel (b) shows the first
286 South African Polar Research Infrastructure (SAPRI) Slocum ocean glider deployments on the
287 eastern Agulhas Bank, representing the first high-resolution sea-glider experiments conducted
288 under SAPRI (d'Hotman et al., 2025). Panel (c) shows a map of ODYSSEA sea surface
289 temperature and GlobCurrent surface currents on 20 July 2017, with the profiling trajectories of
290 the two gliders deployed during the GINA project in 2017 shown in blue and black; white and
291 red symbols indicate glider deployment and recovery locations, respectively (adapted from Krug
292 et al., 2018, EOS). Panel (d) shows satellite-derived sea surface temperature in the Agulhas
293 Current region, with warm waters highlighted in shades of orange illustrating the surface thermal
294 expression of the Agulhas Current (adapted from Krug et al., Council for Scientific and Industrial
295 Research – Natural Resources and the Environment, CSIR-NRE).

296 **2.2. Major developments in satellite remote sensing**

297 Satellite remote sensing has been central to advancing observation of the Greater Agulhas
298 Current System over the past two decades by providing sustained, synoptic coverage of surface
299 ocean properties across spatial and temporal scales that are not achievable with in situ



300 measurements alone. Since 2006, improvements in satellite sensor capabilities, continuity of
301 altimeter missions, and the emergence of multi-sensor products have substantially enhanced the
302 monitoring of sea surface height, surface geostrophic currents, sea surface temperature, winds,
303 and ocean colour across the Agulhas region (Beal et al., 2011; Krug et al., 2010; Pujol et al.,
304 2016). These developments have enabled more detailed characterisation of mesoscale variability,
305 eddy activity, current pathways, and the position and variability of the Agulhas Retroflection,
306 while also supporting investigations of air-sea interaction and ecosystem-relevant surface
307 processes (Johannessen et al., 2014; Krug et al., 2018; Russo et al., 2021).

308
309 The major advance in satellite altimetry over the past two decades has been the availability of
310 continuous, multi-mission, reprocessed SSH products, enabling the derivation of surface
311 geostrophic currents over multi-decadal time scales. The availability of merged, multi-mission
312 altimetry products since the early 1990s, and in particular the release of reprocessed Level-4
313 datasets by the AVISO/DUACS programme, has improved the representation of mesoscale
314 variability, eddy statistics, and current pathways across the Agulhas region (AVISO, 2015; Pujol
315 et al., 2016). These products provide daily fields of SSH and surface geostrophic velocity from
316 1993 onwards, enabling consistent investigation of circulation variability from seasonal to
317 interannual and longer time scales. Over the past decade, the Sentinel continuity missions have
318 contributed to improved spatial and temporal sampling of the ocean surface, strengthening the
319 robustness of merged altimetry products and supporting more detailed analyses of surface
320 circulation features in the Agulhas system (Fig. 4). Improved mapping algorithms and noise-
321 reduction techniques have extended the usefulness of altimetric observations closer to the
322 continental shelf, enhancing the detection and tracking of mesoscale eddies in the Mozambique
323 Channel, south of Madagascar, and along the Agulhas Current and Agulhas Return Current (Halo
324 et al., 2014a; Halo et al., 2014b; Capet et al., 2014; Pujol et al., 2016). Altimetry-based analyses
325 have also advanced quantitative understanding of the mean and variable position of the Agulhas
326 Retroflection, supporting the development of objective methods to identify the core and edges
327 of the Agulhas Current and to assess changes in retroflection behaviour over time (Russo et al.,
328 2021; Russo et al., 2022).

329
330 The launch of the Surface Water and Ocean Topography (SWOT) satellite in 2022 represents a
331 major recent advance in satellite remote sensing, providing the first spaceborne measurements
332 of high-resolution, two-dimensional sea surface height fields. Early analyses using SWOT
333 observations have demonstrated its ability to resolve fine-scale spatial structure in regions of
334 intense mesoscale and submesoscale variability such as the Agulhas Retroflection (Fig. 5). Using
335 data from the fast-sampling phase of the mission, Coadou-Chaventon et al. (2025) showed that
336 conventional nadir altimetry products underestimate the magnitude of surface geostrophic
337 currents in the retroflection region, supporting earlier findings by Hart-Davis et al. (2018), with
338 SWOT-derived velocities exceeding 1 m s^{-1} in localized regions (Fig. 5d,e). To date, two early
339 retroflection events have been identified from SWOT observations, occurring in June 2023 at
340 approximately 25.5°E (Johnson, 2025) and in January 2026 near 22°E . Comparisons of gridded
341 surface fields constructed with and without SWOT data further revealed enhanced representation
342 of fine-scale variability, including submesoscale eddy structure and elevated Rossby numbers in
343 the retroflection region, highlighting the added value of wide-swath altimetry for resolving the
344 detailed surface circulation of the Greater Agulhas Current System (Fig. 5j). Comparisons of
345 gridded surface fields constructed with and without SWOT data further revealed enhanced
346 representation of fine-scale variability, including submesoscale eddy structure and elevated
347 Rossby numbers in the retroflection region, highlighting the added value of wide-swath altimetry
348 for resolving the detailed surface circulation of the Greater Agulhas Current System (Fig. 5j).



349
 350
 351

352

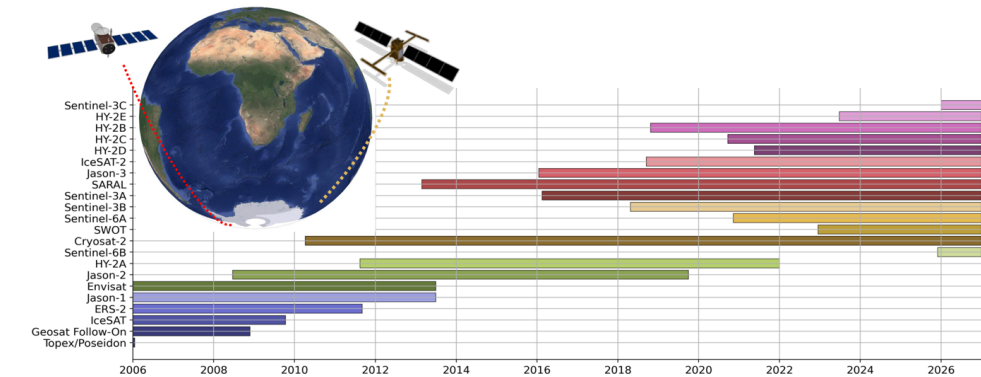
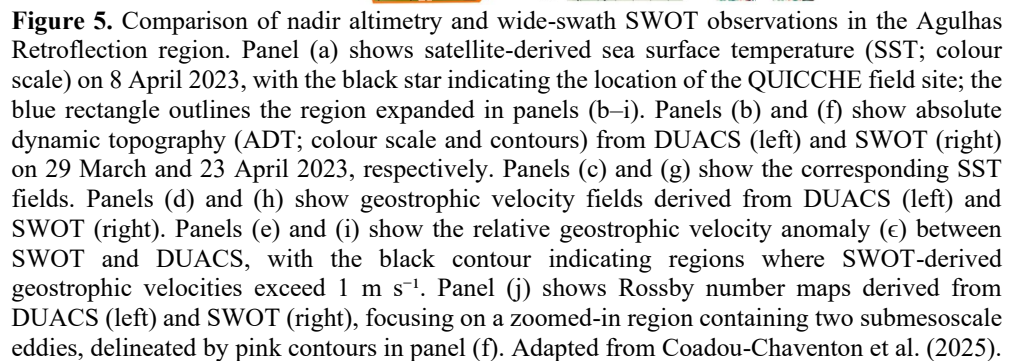


Figure 4. Satellite altimetry temporal coverage over the past two decades.

353



354
 355
 356
 357
 358
 359
 360
 361
 362
 363
 364
 365

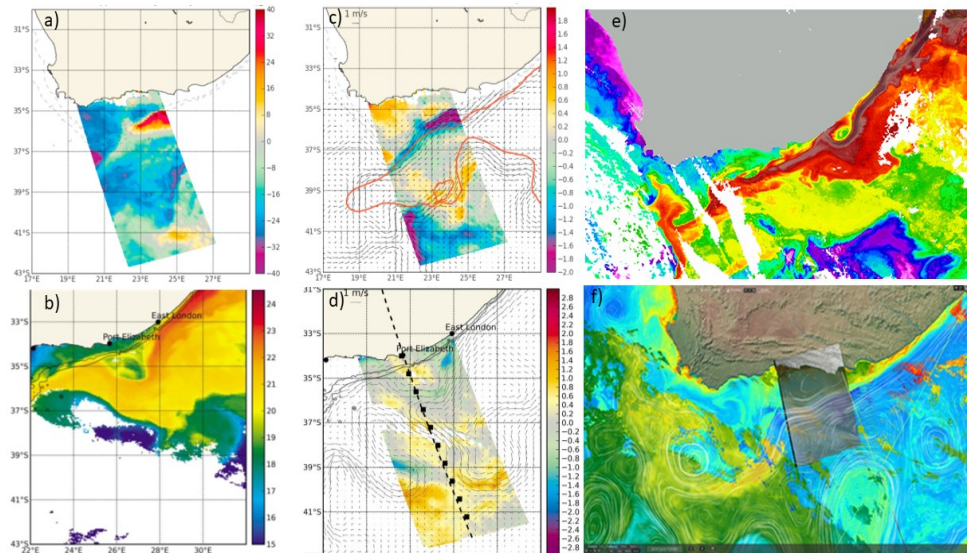
Advances in Synthetic Aperture Radar (SAR) sensing, particularly high-resolution imaging and Doppler-based techniques, have expanded the ability to observe ocean surface currents within the Greater Agulhas Current System by resolving fine-scale surface features associated with strong current gradients, convergence and divergence zones, and air-sea interaction processes. High-resolution SAR imagery has been used to identify surface roughness signatures linked to



371 the Agulhas Current front, mesoscale eddies, and submesoscale features, particularly in regions
372 where intense current shear and frontal activity dominate the surface expression of the flow
373 (Johannessen et al., 2008; Krug et al., 2010). Advances in SAR-based Doppler shift
374 measurements have further enabled retrievals of line-of-sight surface velocities, providing
375 independent estimates of surface current variability that complement geostrophic currents
376 derived from altimetry, including direct comparisons with Lagrangian drifter trajectories (Figure
377 6a,c; Johannessen et al., 2014; Krug et al., 2018). The combined use of SAR Doppler-derived
378 surface velocities and altimetry-based geostrophic currents has enabled detailed assessment of
379 surface flow structure in the Agulhas Current, demonstrating the complementarity of
380 ageostrophic and geostrophic components (Fig. 6a,c).
381

382 Sea surface temperature (SST) observations derived from satellite infrared and microwave
383 sensors have been widely used to characterise the surface expression of the Greater Agulhas
384 Current System, including its frontal structure, mesoscale variability, and interactions with the
385 overlying atmosphere. High-resolution infrared SST imagery has been particularly effective in
386 delineating the Agulhas Current front, tracking mesoscale eddies originating from the
387 Mozambique Channel and south of Madagascar, and documenting variability associated with
388 features such as Natal Pulses (Krug et al., 2010; Weeks et al., 1998), where cold-core structures
389 and associated velocity anomalies are clearly resolved when SST and SAR-derived surface
390 currents are analysed together (Fig. 6b,d). However, the utility of infrared SST observations in
391 the Agulhas region is limited by frequent cloud cover and strong evaporation over the warm
392 current core, which can reduce data availability and introduce biases, particularly in regions of
393 strong thermal gradients (Krug et al., 2010). The combined use of infrared SST with microwave
394 radiometer products and merged altimetry fields has therefore been essential for improving the
395 interpretation of surface thermal variability and its linkage to underlying circulation features
396 (Krug et al., 2010; Imbol et al., 2019). These multi-sensor SST products have also supported
397 investigations of air-sea heat fluxes and mesoscale influences on surface temperature variability
398 in the Agulhas system, highlighting the importance of SST as both a tracer of circulation and a
399 driver of regional air-sea interactions.
400

401 Satellite-derived surface wind observations have contributed to improved understanding of air-
402 sea interactions over the Greater Agulhas Current System, particularly in regions of strong
403 surface currents and sharp thermal fronts. Scatterometer and SAR-based wind products have
404 revealed pronounced spatial variability in wind speed and stress associated with the Agulhas
405 Current, highlighting the modulation of the marine atmospheric boundary layer by underlying
406 oceanic features (Krug et al., 2018). High-resolution SAR observations have shown that wind
407 responses to current-induced surface roughness and SST gradients occur at spatial scales that are
408 not adequately resolved by coarser-resolution scatterometer products, underscoring the
409 importance of fine-scale measurements in this dynamically active region (Johannessen et al.,
410 2014; Krug et al., 2018). Satellite-based estimates of turbulent air-sea fluxes, including latent
411 heat flux, have further demonstrated the ability of high-resolution products to capture the intense
412 exchanges of heat and moisture over the warm Agulhas Current, which play an important role in
413 shaping regional weather and climate variability (Imbol et al., 2019).
414
415



416

417 **Figure 6.** Examples of multi-sensor satellite observations illustrating advances in the retrieval
418 of ocean surface currents and their interaction with thermal and biological surface properties in
419 the Greater Agulhas Current System. Panels (a) and (c) show (a) the ASAR Doppler centroid
420 anomaly (Hz), corrected for along-track variations and land contamination, on 8 May 2008, and
421 (c) the corresponding ASAR-derived range-directed surface current velocity (m s^{-1}), overlaid
422 with geostrophic velocity vectors derived from the CNES-CLS09 mean dynamic topography
423 and the AVISO near-real-time multi-satellite sea level anomaly product. The trajectory of
424 Lagrangian surface drifter 14926 between 9 June and 21 July 2008 is shown in red, and stippled
425 lines indicate the 100 m and 200 m isobaths (adapted from Rouault et al., 2010). Panels (b) and
426 (d) illustrate the passage of a Natal Pulse, showing (b) sea surface temperature from the Meteosat
427 Second Generation sensor, revealing a \sim 150 km diameter cold-core feature at the inshore edge
428 of the Agulhas Current, and (d) ASAR-derived range-directed surface current velocity on 12
429 August 2008, overlaid with AVISO-derived geostrophic velocity vectors. Positive (negative)
430 velocities indicate flow toward the northeast (southwest) (adapted from Rouault et al., 2010).
431 The right-hand panels show examples of integrated multi-sensor products, including sea surface
432 temperature from MODIS, high-resolution Sentinel-1 sea surface roughness modulated by the
433 Agulhas Current, satellite-derived chlorophyll concentration from MODIS and VIIRS, regional
434 ODYSSEA SST, GlobCurrent geostrophic currents, and Jason-2 sea level anomalies (visualised
435 using <https://seascope.oceandatalab.com/data.html/>).

436

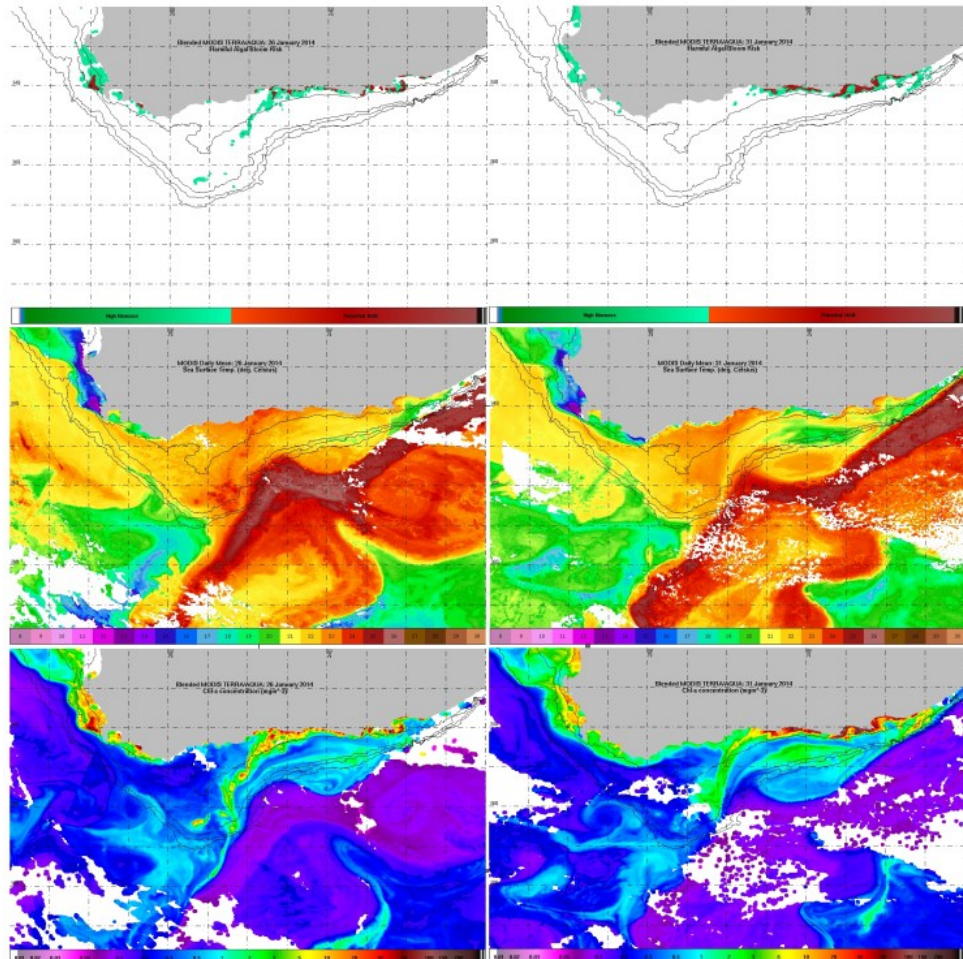
437 Satellite-derived ocean colour observations have provided important insights into the biological
438 expression of variability within the Greater Agulhas Current System by enabling synoptic
439 monitoring of surface chlorophyll-a concentration and related proxies for phytoplankton
440 biomass. In the southern Benguela Upwelling System and across the Agulhas Bank, however,
441 the optical complexity of coastal and shelf waters, particularly during high-biomass and harmful
442 algal bloom (HAB) events, has posed significant challenges for conventional global chlorophyll-a
443 retrieval algorithms based on blue-green band ratios (Matthews et al., 2012; Goyens et al.,
444 2013). Prior to the development of regionally optimised algorithms, satellite observations were
445 unable to resolve the extreme chlorophyll-a concentrations associated with HABs, and pixel data
446 corresponding to bloom conditions were often excluded from analyses, precluding quantitative
447 assessment of bloom extent and intensity (Ryan et al., 2009; Shanmugam, 2012).



447

448 Major advances have since been achieved through the development of regional bio-optical
449 algorithms tailored to the optically complex waters of the southern Benguela and adjacent
450 regions. These include blended approaches that combine blue–green band-ratio algorithms for
451 low to moderate biomass conditions with red to near-infrared band ratios for moderate to high
452 biomass waters, enabling a smooth transition across biomass regimes (Pitcher et al., 2008; Evers-
453 King, 2014; Robertson-Lain et al., 2014). Smith et al. (2018) introduced such an algorithm for
454 the MERIS and OLCI sensors, validated against a wide range of in situ observations,
455 substantially improving the detection and quantification of high-biomass blooms. A similar
456 blended-algorithm approach has subsequently been applied to MODIS data, enabling robust
457 mapping of bloom extent and frequency in the region (Fig. 7). Together, these developments
458 have transformed the utility of satellite ocean colour observations in the Greater Agulhas Current
459 System, allowing quantitative investigation of phytoplankton variability, bloom dynamics, and
460 physical–biological coupling in regions previously considered inaccessible to standard global
461 algorithms.

462



463
464
465
466
467
468
469

Figure 7. Maps of high biomass bloom derived from the improved algorithm blending satellite retrieved information from the blue-green and red to near-infrared parts of the spectrum applied to MODIS data. Top panels show the Harmful Algal Blooms events, middle panels show the corresponding Sea Surface Temperature, and the bottom panels show the chlorophyll-a concentrations. Left panels refers to the HAB event for 20 January 2014 and right panels show the event by 31 January 2014, revealing the events' duration.

470
471
472
473
474
475
476
477
478
479
480

Together, these developments reflect a shift from single-sensor analyses toward integrated, multi-sensor satellite observing frameworks capable of resolving the energetic, multi-scale dynamics of the Greater Agulhas Current System. This transition has been driven not only by the continuity and expansion of satellite missions, but also by major advances in observing geometry, data processing, and algorithm development. In particular, the advent of wide-swath altimetry through the SWOT mission has enabled direct observation of two-dimensional sea surface height variability and fine-scale circulation features that are not resolved by conventional nadir altimetry, while regionally optimised bio-optical algorithms have substantially improved the retrieval of chlorophyll-a concentration in optically complex coastal and shelf waters. These advances, together with improvements in mapping techniques, multi-sensor data integration, and the adoption of free and open-access data policies, including web-based platforms such as the



481 Ocean Virtual Laboratory (<https://ovl.oceandatalab.com/>), have greatly enhanced the ability to
482 co-locate, visualise, and jointly analyse satellite, in situ, and model datasets, thereby
483 strengthening the observational foundation for Agulhas Current research.

484

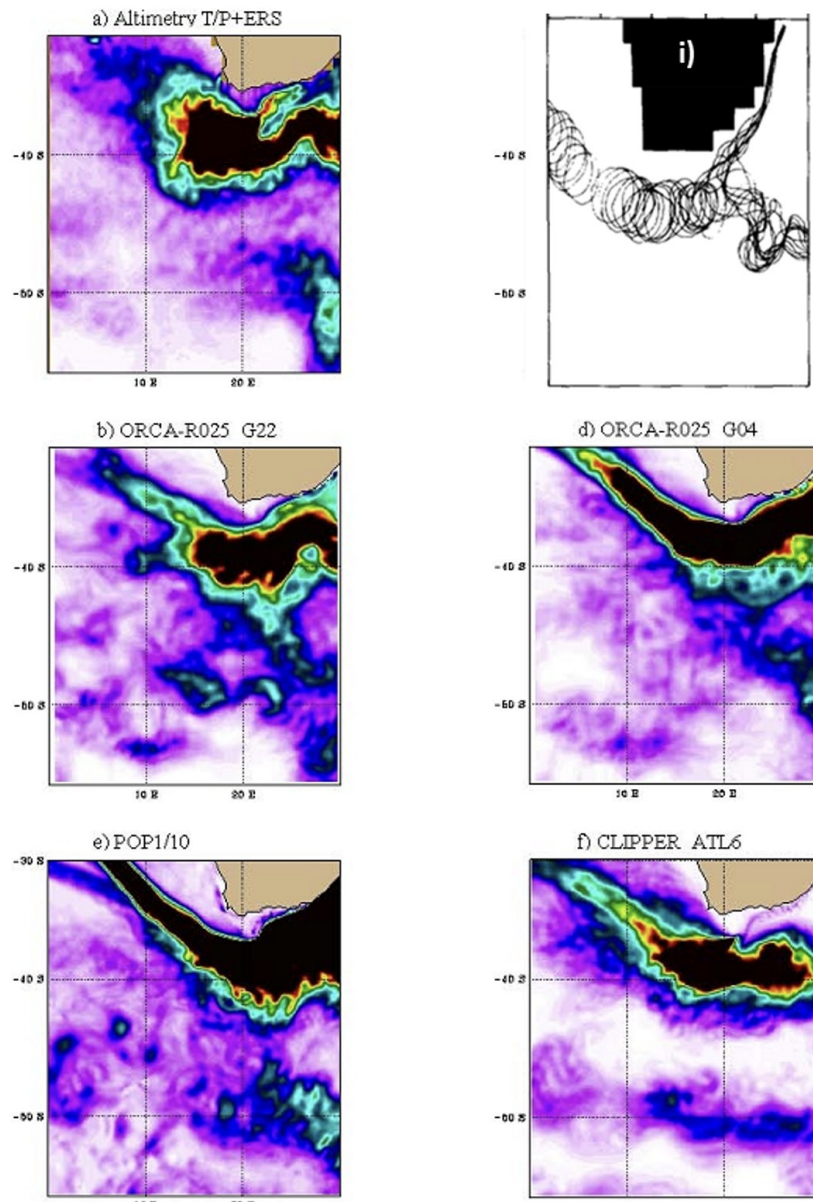
485 **2.3. Major advancements in numerical modelling**

486 Numerical modelling of the Greater Agulhas Current System has a long history, marked by
487 persistent challenges. One of the earliest idealised simulations by Boudra and Chassignet (1988)
488 successfully reproduced a wind-driven South Indian Ocean gyre and captured key features such
489 as the Agulhas Retroflection and ring formation, demonstrating the feasibility of modelling the
490 system at mesoscale-permitting resolution. Subsequent eddy-permitting primitive-equation
491 models, notably the Fine Resolution Antarctic Model (FRAM), reproduced the major elements
492 of the Agulhas system but also revealed systematic deficiencies, including a retroflection
493 occurring too far upstream and eastward, exaggerated mesoscale variability, and Agulhas rings
494 propagating westward along unrealistically straight trajectories (Lutjeharms and Webb, 1995;
495 Figure 8b). These biases were later shown to be remarkably robust across a wide range of model
496 frameworks (e.g. Fig. 8) and resolutions, affecting global and regional configurations, forced and
497 coupled simulations, and even data-assimilative state estimates, including ORCA, POP, OFES,
498 NLOM, HYCOM, ECCO2, and more recent high-resolution coupled climate models such as
499 CESM-HR and AWI-CM-1-1-MR (Maltrud and McClean, 2005; Sasaki et al., 2005; Wallcraft
500 et al., 2002; Thoppil et al., 2011; Zhu et al., 2018; Beech et al., 2022; Großelindemann et al.,
501 2025). In many cases, increasing horizontal resolution alone failed to alleviate, and sometimes
502 exacerbated, these errors, underscoring that accurately representing the Agulhas system requires
503 not only finer resolution but also careful treatment of bathymetry, dissipation, air-sea coupling,
504 and energy pathways. These longstanding challenges have strongly shaped subsequent modelling
505 developments and motivated targeted methodological advances over the past two decades.

506

507 Recognition of systematic biases in early numerical simulations of the Greater Agulhas Current
508 System, together with substantial increases in available computational power, has motivated
509 targeted improvements in numerical formulation, model configuration, and physical process
510 representation. A range of studies demonstrated that addressing the Agulhas retroflection bias
511 requires more than increased horizontal resolution alone, prompting efforts to improve numerical
512 precision and conservation properties, refine bathymetry and dissipation schemes, and better
513 represent key dynamical feedbacks (Barnier et al., 2006; Backeberg et al., 2009; Biastoch and
514 Krauß, 1999; Penven et al., 2006; Loveday et al., 2014). In particular, refining topographic
515 representation and lateral mixing parameters was shown to substantially improve the stability
516 and location of the retroflection in regional model configurations tailored to the Agulhas system
517 (Biastoch and Krauß, 1999; Penven et al., 2006; Biastoch et al., 2008).

518



519
520
521
522
523
524
525
526
527

Figure 8. Example of systematic deficiencies in numerical simulations of the Agulhas Retroflection. The characteristic upstream and eastward displacement of the retroflection, together with exaggerated mesoscale variability, leads to unrealistic patterns of eddy kinetic energy (EKE). The top left panel shows EKE derived from satellite altimetry, used here as a reference. The top right panel shows EKE from the FRAM simulation. The middle panels show results from two ORCA simulations at $\frac{1}{4}^\circ$ resolution, using partial-step bathymetry (left) and full-step bathymetry (right). The bottom panels show EKE from the OPA and Clipper model configurations. Adapted from Barnier et al. (2006).



528 Further advances were achieved by enabling ocean surface current feedbacks on wind stress,
529 which reduced excessive mesoscale variability and stabilised the retroflection, leading to more
530 realistic circulation patterns and leakage pathways (Renault et al., 2017). Collectively, these
531 developments marked a shift from generic eddy-permitting models toward regionally optimised
532 configurations capable of reproducing the observed structure and variability of the Agulhas
533 Current, laying the foundation for subsequent high-resolution and process-oriented modelling
534 studies (Backeberg et al., 2009; Loveday et al., 2014; Schwarzkopf et al., 2019; Penven et al.,
535 2025a).

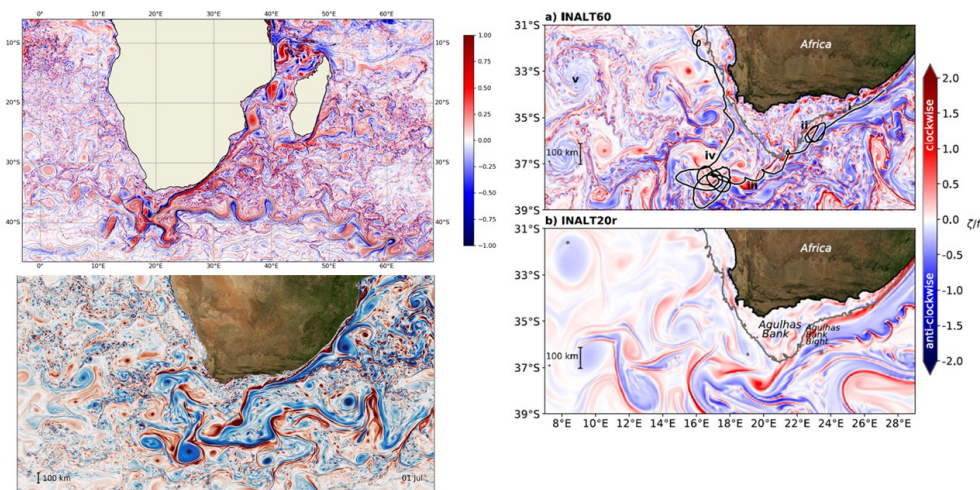
536
537 Many earlier studies of the Agulhas system relied on free-running numerical simulations, despite
538 the strongly nonlinear mesoscale dynamics governing the Agulhas Current and its retroflection
539 and the limited availability of observations to constrain model solutions (Lutjeharms, 2006;
540 Biastoch et al., 2008). Although several global operational data-assimilation systems were
541 available (e.g. MyOcean, BlueLink, and the HYCOM consortium), none were specifically
542 configured for the southern African region, and regionally focused data-assimilation efforts in
543 the Agulhas system had been limited since the work of Evensen and van Leeuwen (1996).
544 Backeberg et al. (2014) explored the use of a regional HYCOM configuration with Ensemble
545 Optimal Interpolation (EnOI) assimilation of along-track satellite sea-level anomaly data. Their
546 results showed that assimilation could improve the consistency of mesoscale eddy placement,
547 reduce eddy kinetic energy errors relative to free-running simulations, and yield modest
548 improvements in subsurface water-mass properties and deep velocities. At the same time, the
549 study emphasised that assimilating anomalies does not correct biases in the model mean state,
550 and that deficiencies in model numerics, forcing, and multivariate relationships can persist in
551 assimilated solutions. These findings reinforced the view that data assimilation alone cannot
552 resolve the long-standing challenges of modelling the Agulhas system, but can provide added
553 value when used alongside continued improvements in model formulation, resolution, and
554 physical realism (Backeberg et al., 2014; Zhu et al., 2018).

555
556 While the modelling advances reviewed here focus primarily on physical circulation, high-
557 resolution simulations have increasingly been used to interpret observed biological and
558 biogeochemical variability in the Agulhas system by linking mesoscale dynamics to nutrient and
559 ecosystem responses. These developments have also highlighted the importance of resolving
560 finer-scale dynamics, as mesoscale-resolving models remain limited in their ability to represent
561 vertical exchanges, frontal processes, and energy pathways that are increasingly recognised as
562 central to Agulhas dynamics.

563
564 Substantial increases in computational power have enabled the development of nested and ultra-
565 high-resolution numerical models capable of explicitly resolving submesoscale dynamics. Using
566 a nested modelling approach achieving horizontal resolutions of order 750 m in the core of the
567 Agulhas Current, Tedesco et al. (2019) demonstrated that shear-driven submesoscale frontal
568 eddies are recurrent features of the current, emerging preferentially during stable phases and
569 modulated by large-scale deformation fields. Similarly, submesoscale-resolving simulations
570 based on the INALT model family, with resolutions down to 1/60°, showed that resolving
571 submesoscale motions enhances the strength, structure, and realism of mesoscale eddies and
572 improves the representation of the Agulhas Retroflection and leakage pathways (Schwarzkopf et
573 al., 2019; Figure 9). These studies further revealed that submesoscale processes reinforce shear-
574 edge eddies and can increase Agulhas leakage by modifying the local balance of instabilities and
575 energy transfers (Schubert et al., 2021). Beyond their impact on circulation pathways,
576 submesoscale-resolving models have enabled new insight into energy cascades within the
577 system, showing that the Agulhas Current acts as a local source of mesoscale energy rather than



578 a net sink, with dissipation pathways varying markedly between the northern and southern
579 segments of the current (Tedesco et al., 2022). Together, these developments demonstrate that
580 explicitly resolving submesoscale dynamics is critical for accurately representing the structure,
581 variability, and energetics of the Agulhas system, and marks a significant advance beyond earlier
582 mesoscale-resolving modelling approaches.
583



584 **Figure 9.** Snapshot of relative vorticity normalised by the planetary vorticity, illustrating the
585 representation of circulation features across a range of spatial scales in numerical simulations of
586 the Greater Agulhas Current System. The left panels show results from high-resolution regional
587 model configurations, with panel (a) from the SWAG36 CROCO simulation (adapted from
588 Penven et al., 2025a) and panel (b) from a NEMO configuration used by Biastoch and
589 Schwarzkopf. The right panels show simulations from the INALT NEMO model at horizontal
590 resolutions of 1/60° and 1/20°, respectively (Schwarzkopf et al., 2019). Across all panels, the
591 models reproduce dominant circulation features of the southern African region at multiple spatial
592 scales, including large-scale currents, mesoscale eddies and rings, and submesoscale meanders
593 and filaments. The influence of submesoscale dynamics in the Agulhas region is highlighted in
594 the zoomed views in the right panels. The black–white line indicates the trajectory of Global
595 Drifter Program drifter 101938, released on 19 February 2013. The extent of the Agulhas Bank
596 is delineated by the 300 m isobath. Key dynamical features are marked, including: (i)
597 submesoscale instabilities along the northern edge of the Agulhas Current; (ii) a shear-edge
598 cyclone in the Agulhas Bank Bight; (iii) a shear-edge cyclone southwest of the Agulhas Bank;
599 (iv) a lee cyclone; and (v) an Agulhas ring surrounded by submesoscale vortices (adapted from
600 Schubert et al., 2022).
601

602 Advances in numerical modelling of the Greater Agulhas Current System over the past two
603 decades reflect a shift from largely exploratory, eddy-permitting simulations toward physically
604 consistent, regionally optimised, and increasingly high-resolution modelling frameworks.
605 Progress has been driven by a combination of increased computational power, improved
606 numerical formulation, refined bathymetry and dissipation schemes, incorporation of air–sea
607 current feedbacks, and, more recently, the explicit resolution of submesoscale dynamics. While
608 persistent challenges remain, particularly in accurately representing the Agulhas Retroflection
609 and leakage across model hierarchies, these developments have substantially improved the
610 realism of simulated circulation, variability, and energetics. Importantly, modelling advances



611 have evolved in close interaction with observational progress, with in situ measurements and
612 satellite products providing essential benchmarks for model evaluation and interpretation, and
613 models, in turn, offering a dynamical framework to integrate disparate observations and test
614 competing hypotheses.

615

616

617 **3. State of knowledge and new insights over the past two decades**

618 Lutjeharms (2006) identified a number of fundamental knowledge gaps spanning all major
619 components of the system, from its upstream source regions to its downstream outflows and
620 global impacts. Many of these gaps related to the structure, variability, and connectivity of the
621 circulation, reflecting the limited observational coverage and modelling capabilities available at
622 the time. Revisiting these unresolved questions provides a coherent framework for assessing
623 progress over the past two decades.

624

625 At the upstream sources of the Agulhas Current, key uncertainties concerned the nature of the
626 circulation through the Mozambique Channel and south of Madagascar. In the Mozambique
627 Channel, long-standing debate focused on whether a spatially continuous southward boundary
628 current exists along the Mozambican coast, or whether the flow is instead dominated by
629 mesoscale eddies. South of Madagascar, similarly fundamental questions were raised regarding
630 the existence and dynamical significance of a retroflection of the South East Madagascar Current
631 and the implications of any eastward return flow in a region dominated by westward wind-driven
632 circulation. Closely related were broader uncertainties surrounding the role of Madagascar as a
633 topographic obstacle shaping current pathways, eddy generation, and connectivity between
634 upstream branches of the Agulhas system.

635

636 Downstream, significant gaps remained in understanding the behaviour and variability of the
637 Agulhas Current and its outflows. For the Agulhas Return Current, questions concerned its
638 interaction with major bathymetric features, its temporal variability, and its role in redistributing
639 waters within the southwest Indian Ocean subtropical gyre. Despite extensive prior research on
640 Agulhas leakage, important uncertainties also persisted regarding the fate and impact of Agulhas
641 rings, including their role in redistributing heat, salt, and vorticity in the South Atlantic, their
642 interaction with the atmosphere, and the extent to which leakage variability is controlled by
643 regional or basin-scale wind forcing.

644

645 The technological and methodological advances outlined in Sect 2 have enabled substantial
646 progress in addressing many of these questions. Expanded in situ observing systems, improved
647 satellite remote sensing, and increasingly realistic numerical models have provided new insight
648 into the structure, variability, and connectivity of the Greater Agulhas Current System across a
649 wide range of spatial and temporal scales. In the following subsections, we revisit each major
650 component of the system in turn. For each region or process, we summarise the state of
651 knowledge up to 2006 and then highlight key advances over the past two decades, drawing on
652 observational, modelling, and interdisciplinary studies to reassess earlier interpretations and
653 identify remaining challenges.

654

655 **3.1. East Madagascar Current and its northern and southern extension**

656 Prior to 2006, understanding of the East Madagascar Current (EMC) and its northern and
657 southern extensions was limited by sparse in situ observations and by differing interpretations of
658 satellite and hydrographic data. The EMC was recognised as the western boundary current of the
659 southwest Indian Ocean subtropical gyre along the eastern margin of Madagascar and as a major
660 upstream contributor to the Greater Agulhas Current System (Lutjeharms, 2006). However, its



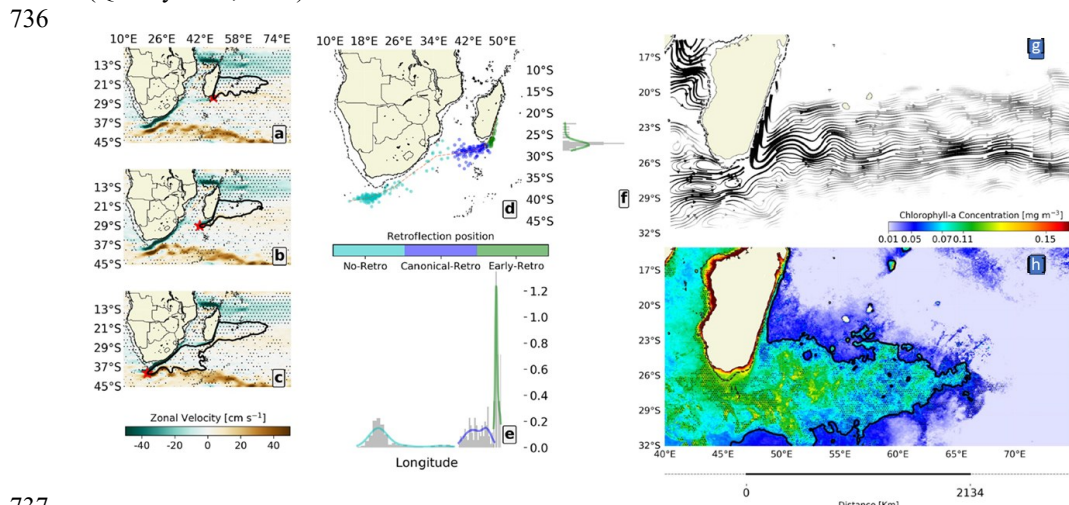
661 mean structure, transport, variability, and downstream connectivity remained poorly constrained,
662 particularly relative to better-studied western boundary currents elsewhere.
663
664 At its northern extent, the EMC was understood to be fed primarily by the westward-flowing
665 South Equatorial Current (SEC), which bifurcates upon encountering Madagascar (Lutjeharms,
666 2006). The partitioning of this flow around the island was recognised as an important control on
667 the volume and properties of waters entering the Mozambique Channel and, ultimately, the
668 Agulhas Current. Nevertheless, the relative importance of a continuous boundary current along
669 eastern Madagascar versus episodic transport mediated by mesoscale eddies and filaments
670 remained uncertain, owing to the lack of sustained direct velocity measurements along the
671 margin (Lutjeharms, 2006; de Ruijter et al., 2004).
672
673 South of Madagascar, the behaviour of the southern extension of the EMC was particularly
674 contentious. A central unresolved question was whether the EMC undergoes a retroflexion south
675 of the island, forming an eastward return flow, or whether it primarily feeds westward into the
676 Mozambique Channel and the Agulhas Current without a coherent turning. Early interpretations
677 based largely on satellite altimetry, drifter trajectories, and limited hydrographic sections
678 suggested the existence of a retroflective pathway (e.g. Siedler et al., 2006), but these
679 interpretations were challenged on dynamical grounds. In particular, an eastward return flow
680 would oppose the generally westward wind-driven circulation of the region, leading some
681 authors to question its physical plausibility and to refer to the proposed feature as a “retro-fiction”
682 (Quartly et al., 2006).
683
684 Adding to this ambiguity was the identification of the South Indian Counter Current (SICC), an
685 eastward-flowing current embedded within the subtropical gyre south of Madagascar. Although
686 the SICC was formally described only in the mid-2000s (Palastanga et al., 2006; Siedler et al.,
687 2006), its presence complicated interpretation of eastward flows inferred from satellite data. In
688 particular, it raised the possibility that some observations previously attributed to a retroflecting
689 EMC might instead reflect the broader gyre-scale circulation associated with the SICC
690 (Lutjeharms, 2006; Quartly et al., 2006). Distinguishing between a true southern EMC return
691 flow and the SICC thus remained a major challenge prior to 2006.
692
693 The degree of connectivity between the EMC, its southern extension, and downstream pathways
694 also remained unresolved. It was unclear whether the EMC connects continuously to the Agulhas
695 Current via the Mozambique Channel, or whether this connection is intermittently disrupted by
696 the shedding of mesoscale eddies, dipoles, and filaments south of Madagascar (de Ruijter et al.,
697 2004; Siedler et al., 2009). The role of Madagascar’s complex topography in steering the flow,
698 generating mesoscale variability, and modulating these connections was recognised as
699 potentially important but poorly quantified, motivating early sensitivity experiments using
700 regional numerical models (Penven et al., 2006).
701
702 Additionally, prior to 2006, biogeochemical and ecosystem characteristics of the East
703 Madagascar Current and its extensions were largely unexplored, with understanding of
704 biological variability limited to indirect inferences from physical circulation and mesoscale
705 activity, reflecting the scarcity of targeted observations in the region (Lutjeharms, 2006).
706
707 Since 2006, targeted in situ observations, improved satellite analyses, and high-resolution
708 numerical modelling have substantially clarified the structure, variability, and downstream
709 connectivity of the East Madagascar Current (EMC).
710



711 Sustained mooring observations south of Madagascar, deployed as part of the INdian–ATlantic
712 Exchange (INATEX) programme, provided the first direct time series of velocity and transport
713 variability of the EMC and its undercurrent (Ullgren et al., 2012; Ponsoni et al., 2015; Ponsoni
714 et al., 2016). These measurements demonstrated that the EMC is a coherent, vertically structured
715 boundary current with substantial variability on seasonal to interannual time scales, and that a
716 significant fraction of its transport is carried below the surface. The observations further showed
717 that the EMC does not form a steady downstream pathway, but instead interacts strongly with
718 mesoscale eddies south of Madagascar.

719
720 Satellite altimetry and eddy-tracking analyses confirmed that the southern extension of the EMC
721 is embedded in an energetic eddy field characterised by frequent shedding of cyclonic and
722 anticyclonic eddies (Halo et al., 2014a; Halo et al., 2014b). These eddies intermittently divert
723 EMC waters westward toward the Mozambique Channel or eastward into the subtropical gyre,
724 reconciling earlier conflicting interpretations of continuous versus intermittent connectivity to
725 the Agulhas system (de Ruijter et al., 2004; Siedler et al., 2009).

726
727 The long-standing debate regarding a retroflection of the EMC south of Madagascar has also
728 been resolved. Observational and modelling studies have shown that while eastward flow occurs
729 in this region, it is more accurately attributed to the South Indian Counter Current (SICC) rather
730 than a persistent retroflection of the EMC itself (Siedler et al., 2009; Ramanantsoa et al., 2021).
731 Satellite altimetry analyses have further demonstrated that the southern extension of the EMC
732 exhibits distinct retroflection regimes with preferred longitudinal and latitudinal positions, rather
733 than a single fixed retroflection point (Fig. 10). This distinction clarified earlier ambiguities
734 arising from satellite-based interpretations and effectively closed the “retro-fiction” debate
735 (Quarry et al., 2006).



737
738 **Figure 10.** Spatial variability of the southern extension and retroflection of the South East
739 Madagascar Current (SEMC) inferred from satellite altimetry. Panels a to c show composites of
740 SEMC retroflection positions derived from satellite sea surface height (SSH). The black contour
741 outlines the SEMC and its retroflection, while red stars indicate the westernmost point of the
742 selected SSH contour, used here as a proxy for the retroflection location. Background shading
743 shows composites of zonal surface velocity corresponding to each retroflection regime. Hatched
744 black dots denote regions where anomalies are significant at the 95% confidence level based on
745 a two-tailed Student's t-test. Panel (d) presents the spatial classification of SEMC retroflection



746 positions obtained using unsupervised k-means clustering, with the dotted red line indicating the
747 most likely retroflection location. Each classified retroflection case is used to construct the
748 composites shown in panels a to c. Panel (e) shows the longitudinal distributions of the three
749 identified retroflection regimes, while panel (f) shows the corresponding latitudinal distribution
750 for the early retroflection case. Adapted from Ramanantsoa et al. (2021).

751
752 High-resolution regional modelling has further elucidated the dynamical controls on EMC
753 variability and connectivity. Numerical experiments demonstrated that Madagascar's
754 topography plays a central role in steering the flow, generating mesoscale variability, and
755 regulating the partitioning of transport between the Mozambique Channel and downstream
756 branches of the Agulhas system (Penven et al., 2006; Halo et al., 2014a). Energy conversion
757 analyses revealed the coexistence of barotropic and baroclinic instabilities south of Madagascar,
758 with spatially distinct regimes influencing eddy generation and downstream transport pathways
759 (Halo et al., 2014b). More recent ultra-high-resolution simulations have highlighted strong
760 vertical and seasonal variability in boundary currents and thermal fronts along shelves and island
761 wakes, further refining understanding of EMC dynamics (Sudre et al., 2023; Penven et al.,
762 2025a).

763
764 Emerging interdisciplinary studies have also begun to link physical variability in the EMC region
765 to ecosystem responses. Mesoscale eddies south of Madagascar have been shown to influence
766 nutrient distributions and biological productivity, structuring ecosystems from phytoplankton to
767 top predators (Weimerskirch et al., 2004; Barlow et al., 2014). While still limited in scope, these
768 studies represent a shift beyond the predominantly physical focus of pre-2006 research.

769
770 The East Madagascar Current is now considered to be a dynamically complex and intermittently
771 connected component of the Greater Agulhas Current System. Although important questions
772 remain regarding long-term variability and climate sensitivity, the fundamental structure and
773 downstream role of the EMC are now substantially better understood than prior to 2006.

774 **3.2. Mozambique Channel**

775
776 The Mozambique Channel (MC) has historically been recognised as a key upstream source
777 region of the Agulhas Current, yet it remained one of the least well constrained components of
778 the Greater Agulhas Current System because of sparse in situ observations and strong mesoscale
779 variability (Lutjeharms, 2006). Early conceptual models had postulated the existence of a
780 persistent, spatially continuous southward boundary current along the Mozambican coast—the
781 so-called Mozambique Current—but this hypothesis was increasingly questioned in the early
782 2000s.

783
784 Analyses combining hydrographic observations, direct current measurements, and satellite
785 altimetry provided evidence that a coherent, continuous Mozambique Current does not exist.
786 Instead, the circulation of the MC was shown to be dominated by large mesoscale eddies that
787 propagate poleward through the channel and intermittently feed the Agulhas Current (de Ruijter
788 et al., 2002; Ridderinkhof and de Ruijter, 2003). These findings fundamentally altered prevailing
789 views of MC dynamics and suggested that upstream forcing of the Agulhas Current is highly
790 variable in time, governed largely by eddies rather than by steady boundary flow (Lutjeharms,
791 2006).

792
793 Despite this conceptual advance, substantial uncertainty remained regarding the detailed
794 structure and dynamics of the MC eddy field. Anticyclonic eddies were widely considered the
795 dominant mesoscale feature, but the presence and significance of cyclonic eddies was disputed.



796 In particular, it was argued that apparent cyclonic features identified in altimetric products could
797 arise from artefacts associated with temporal averaging of sea-level anomaly fields rather than
798 from persistent dynamical structures (de Ruijter et al., 2002). As a result, the full spectrum of
799 eddy types, their generation mechanisms, and their vertical structure remained poorly resolved.
800

801 Connectivity between the MC and downstream components of the Agulhas system was also
802 incompletely understood. While eddy propagation through the channel was recognised as a
803 primary pathway linking the MC to the Agulhas Current, the degree to which this connection
804 was continuous versus intermittent remained uncertain (de Ruijter et al., 2004; Lutjeharms,
805 2006). Questions persisted regarding how eddies interacted with channel bathymetry and the
806 continental slope, how frequently they merged with or reinforced the Agulhas Current, and how
807 reliably these processes could be inferred from the limited observational record available at the
808 time.
809

810 By 2006, therefore, the Mozambique Channel was viewed as an energetic, eddy-dominated
811 source region whose influence on the Agulhas Current was fundamentally intermittent rather
812 than steady (de Ruijter et al., 2002; Ridderinkhof and de Ruijter, 2003; Lutjeharms, 2006).
813 However, key aspects of the MC circulation—including the persistence of any mean boundary
814 flow, the role of cyclonic versus anticyclonic eddies, and the sensitivity of MC variability to
815 atmospheric and remote forcing—remained unresolved. These uncertainties were explicitly
816 identified as priorities for future observational and modelling efforts aimed at quantifying the
817 role of the MC within the Greater Agulhas Current System (Lutjeharms, 2006).
818

819 Over the past two decades, a combination of sustained in situ observations, improved satellite
820 analyses, and high-resolution numerical modelling has fundamentally advanced understanding
821 of circulation and variability in the Mozambique Channel (MC). These efforts have confirmed
822 the eddy-dominated nature of the flow while resolving long-standing uncertainties regarding
823 eddy populations, generation mechanisms, and downstream connectivity to the Agulhas Current.
824

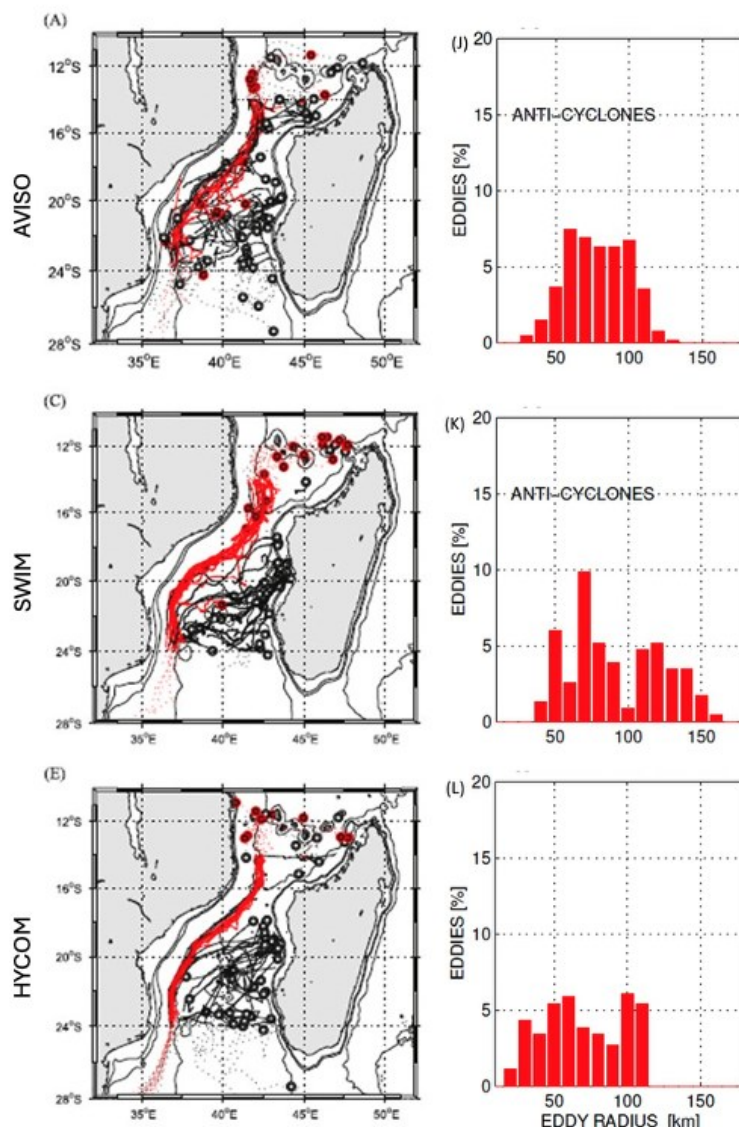
825 The most significant observational advance has been the deployment of long-term mooring
826 arrays in the MC, most notably the Long-term Ocean Climate Observation (LOCO) array. These
827 sustained measurements provided the first continuous time series of velocity, temperature, and
828 salinity across the channel, demonstrating unequivocally that the mean flow is not organised as
829 a persistent boundary current but is instead dominated by strong mesoscale variability (Ullgren
830 et al., 2012). The LOCO observations quantified the transport associated with individual eddies
831 and revealed substantial variability on intraseasonal to interannual time scales, directly
832 confirming interpretations previously inferred from satellite altimetry.
833

834 High-resolution satellite altimetry and eddy-tracking analyses have further refined understanding
835 of the MC eddy field. These studies demonstrated that the channel hosts a diverse population of
836 mesoscale eddies, including both anticyclonic and cyclonic structures, overturning earlier
837 suggestions that cyclonic eddies were merely artefacts of data processing (Halo et al., 2014a).
838 Eddy trajectories derived from altimetry showed consistent southwestward propagation
839 pathways, with many eddies maintaining coherent structure over several months as they transit
840 the channel and interact with the continental slope (Fig. 11; Halo et al., 2014a; Halo et al., 2014b).
841 These results clarified how MC eddies intermittently feed the Agulhas Current and contribute to
842 its variability.
843

844 Regional numerical modelling has played a central role in interpreting these observations and
845 identifying the dynamical mechanisms governing MC variability. High-resolution simulations



846 using ROMS_AGRIF, including the South West Indian Ocean Model (SWIM), successfully
847 reproduced observed eddy trajectories, sizes, and lifetimes, lending confidence to their
848 representation of MC dynamics (Fig. 11, middle panels; Halo et al., 2014a). Energy conversion
849 analyses from these simulations revealed a coexistence of barotropic and baroclinic instabilities
850 in the region, with spatially distinct regimes influencing eddy generation north and south of
851 Madagascar (Halo et al., 2014b). More recent ultra-high-resolution simulations have further
852 highlighted the strong vertical structure of MC eddies and their seasonal modulation, particularly
853 along continental shelves and island wakes (Sudre et al., 2023; Penven et al., 2025a).
854



855
856 **Figure 11.** Eddy trajectories and size distributions in the Mozambique Channel derived from
857 observations and numerical models. Left panels show eddy tracks identified from satellite



858 altimetry (AVISO; top), the SWIM regional model simulation (middle), and the HYCOM
859 simulation (bottom). Red trajectories highlight large anticyclonic Mozambique Channel rings
860 with radii exceeding 100 km. Right panels show the corresponding probability density
861 distributions of eddy radii for each dataset, binned in 10 km intervals. Adapted from Halo et al.
862 (2014a).

863 Beyond physical circulation, post-2006 observational and modelling efforts have substantially
864 advanced understanding of how mesoscale variability in the Mozambique Channel influences
865 biological productivity and ecosystem structure. Regional multidisciplinary programmes,
866 including ACEP, ASCLME, MESOP, MESOBIO, MadRidge, WIOURI, and RESILIENCE,
867 have generated a growing body of hydrographic, biological, and biogeochemical observations
868 that allow physical drivers of ecosystem variability in the Mozambique Channel and south of
869 Madagascar to be more clearly identified (Vousden et al., 2012; Barlow et al., 2014; Halo et al.,
870 2017). These studies consistently demonstrate that mesoscale eddies play a central role in
871 structuring nutrient distributions, phytoplankton biomass, and higher trophic-level responses in
872 the source regions of the Agulhas Current.

873 Coupled physical–biogeochemical modelling experiments using ROMS_AGRIF with the
874 PISCES ecosystem model, developed within the MESOBIO programme, further underscored the
875 importance of eddy history, topographic interactions, and lateral advection of coastal waters in
876 shaping regional productivity patterns (José et al., 2014, 2016). These simulations showed that
877 eddy-driven offshore transport of nutrient-rich coastal waters can enhance offshore productivity
878 while simultaneously reducing nutrient availability near the coast, highlighting the dual role of
879 mesoscale variability in redistributing biogeochemical resources. Similar conclusions have
880 recently been corroborated by long-term, high-resolution simulations using the coupled
881 CROCO–PISCES system, which further emphasised the persistence of eddy-driven modulation
882 of productivity at seasonal to interannual time scales (Chenillat et al., 2024).

883 Along the Mozambican shelf, particularly over the Sofala Bank, ship based observations and
884 high-resolution regional modelling have revealed a strong coupling between shelf dynamics,
885 mesoscale variability, and ecosystem processes. The Sofala Bank supports a major penaeid
886 shrimp fishery and is characterised by intense tidal currents, with barotropic velocities reaching
887 40–70 cm s⁻¹, giving rise to distinct inshore, shelf-break, and offshore hydrographic regimes
888 (Chevane et al., 2016). High-resolution modelling studies indicate that mesoscale eddies
889 modulate shelf circulation, hydrography, and the structure of river plumes, notably the
890 bidirectional Zambezi River plume, although wind forcing and river discharge also exert a strong
891 influence (Nehama and Reason, 2015; Malauene et al., 2018). Lagrangian individual-based
892 modelling of shrimp larval dispersal further suggests that mesoscale eddies can have both
893 detrimental and beneficial ecosystem impacts, with cold-core cyclonic eddies increasing larval
894 mortality rates while simultaneously enabling long-distance dispersal and enhancing regional
895 population connectivity (Malauene et al., 2024).

896 The Delagoa Bight is an ecologically and economically important shelf region off southern
897 Mozambique, characterised by enhanced chlorophyll-a concentrations relative to adjacent open-
898 ocean waters (Lutjeharms, 2006; Quartly and Srokosz, 2004). Circulation is dominated by a
899 quasi-permanent cyclonic eddy trapped within the Bight, which promotes isopycnal doming,
900 nutrient supply to the euphotic zone, and retention of biological productivity (Lutjeharms, 2006;
901 Lamont et al., 2010; Cossa et al., 2016). Nearshore observations off Inhaca Island show strong
902 seasonal variability, with maximum temperatures in austral summer and minima in winter, and
903 elevated nutrients and reduced salinity associated with increased summer river discharge (Paula
904



907 et al., 1998). Despite this, nearshore chlorophyll-a and zooplankton abundances are generally
908 low, with seasonal peaks in September and March–April, suggesting that hydrographic
909 conditions rather than river input dominate phytoplankton biomass variability across the Bight
910 (Paula et al., 1998; Kyewalyanga et al., 2007). Early in situ studies reported chlorophyll-a
911 concentrations of 0.6–1.26 mg m⁻³ and primary production rates of 0.6–1.0 g C m⁻² day⁻¹ or
912 higher, indicative of mesotrophic conditions, with diatoms dominating cooler, nutrient-rich
913 waters in the northeast and smaller flagellates elsewhere (Mitchell-Innes, 1967; Ryther et al.,
914 1966; Mordasova, 1980; Barlow et al., 2008; Sá et al., 2013). However, observations remain
915 sparse, satellite chlorophyll-a substantially underestimates in situ values, and the spatial and
916 temporal variability of plankton biomass and its response to oceanographic forcing in the
917 Delagoa Bight remain poorly quantified (Kyewalyanga et al., 2007; Lamont et al., 2018; Tew-
918 Kai and Marsac, 2009).

919
920 With these findings, the channel is now recognised not only as an eddy-dominated dynamical
921 source region of the Agulhas Current, but also as a region where physical–biological coupling
922 strongly shapes productivity, fisheries, and connectivity at regional scales.

923
924 **3.3. Northern Agulhas Current**

925 Early hydrographic surveys, current-meter measurements, and satellite observations established
926 the Northern Agulhas Current (NAC) as a narrow, intense western boundary current flowing
927 southwestward along the southeast African continental margin (Gründlingh, 1979; Gründlingh,
928 1986; Lutjeharms and Valentine, 1988). The current was shown to be strongly constrained by
929 the steep continental slope, resulting in a comparatively stable mean path relative to other
930 western boundary currents, with limited lateral meandering over most of its upstream extent
931 (Beal and Bryden, 1997; Beal and Bryden, 1999). Surface velocities frequently exceeded 2 m s⁻¹
932 on the inshore edge of the current, and hydrographic sections revealed a strongly baroclinic
933 structure with a warm, saline surface core overlying cooler intermediate waters (Gründlingh,
934 1986; Beal and Bryden, 1997).

935
936 Transport estimates derived from ship based sections indicated that the NAC carries the majority
937 of the volume transport within the Greater Agulhas Current System, with values increasing
938 downstream as additional source waters are incorporated (Beal and Bryden, 1999). However, the
939 sparsity of repeated sections limited the ability to quantify temporal variability in transport or to
940 resolve changes on seasonal to interannual time scales.

941
942 Mesoscale variability in the NAC was recognised as being spatially heterogeneous, with the
943 Natal Bight identified as a key region of enhanced instability. In this region, the widening of the
944 continental shelf permits the development of large offshore meanders known as Natal Pulses
945 (Gründlingh, 1979; Lutjeharms and Roberts, 1988). These features propagate downstream at
946 rates of approximately 10–20 km day⁻¹ and are associated with deep-reaching cyclonic eddies
947 embedded within the meander structure (Gründlingh and Pearce, 1984; Lutjeharms and Connell,
948 1989). Natal Pulses were recognised as the dominant expression of mesoscale variability in the
949 NAC and were hypothesised to modulate downstream circulation, including the stability of the
950 Agulhas Retroflection (Lutjeharms and van Ballegooyen, 1988; van Leeuwen et al., 2000).

951
952 Interactions between the NAC and the continental shelf were acknowledged as dynamically
953 important but remained poorly constrained prior to 2006. Observations indicated intermittent
954 shelf-edge upwelling, shear-edge eddies, and cross-shelf exchange, particularly in the Natal
955 Bight and near Cape St Lucia (Gill and Schumann, 1979; Schumann, 1987; Lutjeharms and



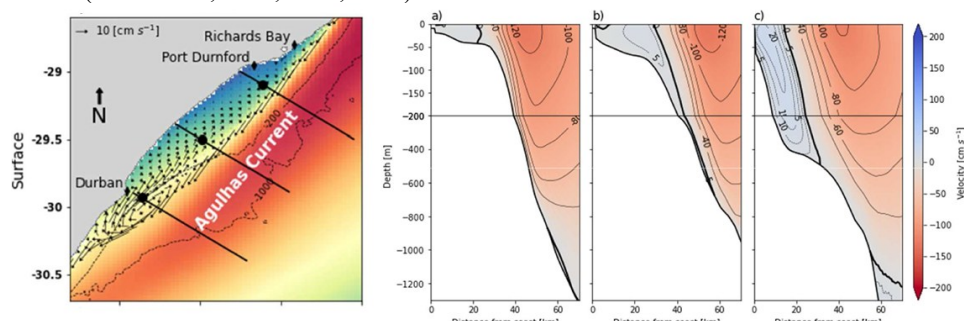
956 Meeuwis, 1987). However, the frequency, spatial structure, and driving mechanisms of these
957 processes were difficult to resolve from the limited observational record available at the time.
958

959 Since 2006, sustained observations and improved satellite products have enabled the Northern
960 Agulhas Current to be described in terms of its time-varying structure rather than only its mean
961 path. Multi-year altimetric analyses provided new perspectives on the occurrence, surface
962 expression, and propagation of Natal Pulses (Krug and Penven, 2011), while longer, more
963 consistent records revealed a robust annual cycle in the Agulhas Current signal that had not been
964 quantified previously (Krug and Tournadre, 2012). Parallel advances in satellite current
965 retrievals, supported by comparisons with observed and virtual drifters, improved confidence in
966 diagnosing surface variability along the Agulhas Current pathway (Krug et al., 2010; Hart-Davis
967 et al., 2018).

968 A major advance has been the ability to observe and interpret the inshore edge of the current at
969 much finer scales. The first buoyancy-glider deployments within the Agulhas Current revealed
970 the ubiquitous presence of shear-generated submesoscale cyclonic eddies along the inshore
971 boundary, demonstrating that energetic submesoscale variability is a persistent feature of the
972 system (Krug et al., 2017). Subsequent glider experiments further resolved the fine-scale
973 structure of the inshore front and quantified turbulence and mixing processes that are not
974 captured by conventional moorings or standard satellite products (Krug et al., 2018; Pringle et
975 al., 2022).

976 Recent observations combining satellite altimetry and surface drifters showed that mesoscale
977 eddies originating from the Mozambique Channel and south of Madagascar typically dissipate
978 upon approaching the northern Agulhas Current, transferring momentum to the boundary current
979 rather than remaining coherent features. Anticyclonic eddies were found to locally accelerate the
980 current core, while cyclonic eddies weaken the flow and promote offshore meanders, frequently
981 associated with the development of Natal Pulses, highlighting the northern Agulhas Current as a
982 significant sink of eddy kinetic energy (Braby et al., 2016).

983 Post-2006 research has also sharpened understanding of coastal and shelf circulation features
984 adjacent to the NAC. Modelling studies identified the Natal Bight Coastal Counter-Current as a
985 dynamically significant inshore flow, providing new insight into shelf-boundary current
986 interactions and their variability (Fig. 12; Heye et al., 2022). In addition, targeted observational
987 and modelling studies along the northeast South African margin, including Sodwana Bay, refined
988 the role of bathymetry, mesoscale eddies, and upwelling processes in driving episodic cold-water
989 events (Wells et al., 2021, 2024, 2025).



993
994 **Figure 12.** Model-derived mean surface circulation in the Natal Bight region, showing the
995 northward-flowing Natal Bight Coastal Counter-Current (NBC3) inshore of the southward-



996 flowing Agulhas Current. Black transect lines indicate the locations at which cross-shelf vertical
997 sections of alongshore velocity were extracted. Panels (a–c) show the corresponding vertical
998 sections for the northern, central, and southern transects, respectively. Adapted from Heye et al.
999 (2022).

1000 Beyond physical circulation, post-2006 observational programmes have substantially improved
1001 understanding of productivity and biogeochemical variability inshore of, and within, the
1002 Northern Agulhas Current. Ship based surveys along the Agulhas System Climate Array (ASCA)
1003 revealed that, despite its warm and saline character, the Agulhas Current supports levels of net
1004 primary production comparable to other western boundary currents, particularly during winter,
1005 with reported rates of $34\text{--}82 \text{ mmol C m}^{-2} \text{ d}^{-1}$ (Sinyanya et al., 2024). Enhanced productivity was
1006 consistently associated with mesoscale features, indicating that meanders, eddies, and frontal
1007 processes play a central role in nutrient supply to the euphotic zone. Satellite-based global
1008 primary production products yield similar ranges (Huang et al., 2021), although limited in situ
1009 observations constrain robust validation.

1010
1011 Recent studies further highlighted the role of the Agulhas Current as a conduit for
1012 biogeochemical signals originating in the tropical Indian Ocean. The warm, low-nutrient
1013 environment of the current provides favourable conditions for nitrogen fixation, with estimated
1014 N_2 -fixation rates of $7\text{--}25 \text{ Tg N yr}^{-1}$ across the greater Agulhas region (Marshall et al., 2023),
1015 contributing up to $\sim 5\%$ of primary production during wintertime observations (Sinyanya et al.,
1016 2024). The isotopic imprint of nitrogen fixation has been proposed as a potential tracer of
1017 Agulhas water masses and their leakage into the South Atlantic (Granger et al., 2024).

1018
1019 Finally, new satellite-based and modelling studies have strengthened evidence that the Northern
1020 Agulhas Current is a regional air–sea interaction hotspot. High-resolution remote sensing
1021 analyses quantified the intensity and variability of latent heat fluxes over the current (Imbol et
1022 al., 2019), while modelling studies demonstrated that Agulhas Current variability can influence
1023 southern African precipitation, reinforcing the climate relevance of mesoscale SST and surface-
1024 flux anomalies associated with the NAC (Imbol et al., 2021).

1025 3.4. Southern Agulhas Current

1026 The Southern Agulhas Current (SAC), extending from approximately 34°S to the southern tip of
1027 Africa, has long been recognised as a dynamically distinct segment of the Agulhas Current
1028 system, exhibiting substantially enhanced variability relative to its northern counterpart. Early
1029 hydrographic surveys, current-meter measurements, and satellite observations demonstrated that
1030 as the current flows over the widening continental shelf and complex bathymetry of the Agulhas
1031 Bank, topographic steering weakens and mesoscale activity intensifies (Gründlingh, 1983;
1032 Lutjeharms and Roberts, 1988). This transition manifests as frequent meanders, filaments, and
1033 eddy formation, particularly along the inshore edge of the current.

1034
1035 Prior to 2006, studies showed that large-amplitude meanders generated along the southern
1036 segment can propagate downstream and strongly influence the stability and behaviour of the
1037 Agulhas Retroflection (Lutjeharms and van Ballegooyen, 1988; van Leeuwen et al., 2000). These
1038 findings established a causal link between SAC variability and retroflection instability,
1039 highlighting the importance of the southern current in preconditioning inter-ocean exchange.
1040 Hydrographic sections further confirmed that the SAC remains strongly baroclinic, with
1041 transport estimates broadly consistent with upstream values but exhibiting increased temporal
1042 variability (Gordon et al., 1987; Beal and Bryden, 1997, 1999). However, the episodic nature of
1043 these observations limited the ability to resolve seasonal to interannual variability.



1045

1046 Interactions between the SAC and the Agulhas Bank shelf were also recognised early as
1047 dynamically and ecologically important. Observations revealed episodic shelf-edge upwelling,
1048 cross-shelf exchange, and enhanced retention of shelf waters driven by current meanders,
1049 cyclonic eddies, and filaments (Boyd et al., 1992; Lutjeharms et al., 2000). Sea surface
1050 temperature analyses highlighted strong thermal variability across the Bank, reflecting the
1051 interplay between the Agulhas Current, shelf bathymetry, and atmospheric forcing (Shillington,
1052 1998). Biological studies conducted prior to 2006 provided early evidence of physical–biological
1053 coupling, with enhanced phytoplankton biomass and primary production observed during
1054 upwelling events and periods of intensified mesoscale activity (Probyn et al., 1994; Pitcher et
1055 al., 1998). Despite these insights, the frequency, magnitude, and persistence of SAC-driven shelf
1056 processes remained poorly constrained due to limited temporal coverage.

1057

1058 Since 2006, high-resolution satellite altimetry and sea surface temperature analyses have
1059 demonstrated that mesoscale activity intensifies markedly downstream of the Agulhas Bank,
1060 with frequent large-amplitude meanders, filaments, and eddy shedding events (e.g. Fig. 7 middle
1061 panels; Krug et al., 2010; Russo et al., 2021). These datasets revealed coherent spatial patterns
1062 and temporal variability that were not resolvable from earlier synoptic observations,
1063 strengthening links between SAC variability, shelf interactions, and downstream circulation
1064 changes. Targeted process studies further refined understanding of shelf–slope exchange
1065 mechanisms. Using satellite observations combined with in situ measurements from autonomous
1066 platforms, Krug et al. (2014) showed that interactions between the Agulhas Current and the
1067 eastern margin of the Agulhas Bank drive strong, spatially structured cross-shelf exchange
1068 mediated by meanders, cyclonic eddies, and frontal instabilities. Along the Transkei shelf,
1069 similar interactions alternately induce upwelling and downwelling, uplifting nutrient-rich South
1070 Indian Central Water onto the shelf during meandering events while promoting offshore export
1071 during downwelling phases (Goschen et al., 2015; Lamont et al., 2016; Russo et al., 2019;
1072 Lamont et al., 2024a). Individual meanders differ substantially in their hydrographic impact,
1073 leading to pronounced spatial heterogeneity in physical and biological responses along the shelf
1074 (Russo et al., 2019).

1075

1076 The enhanced dynamical variability of the SAC has strong ecological and biogeochemical
1077 consequences, particularly along the Transkei shelf and the Agulhas Bank. Mesoscale meanders
1078 have been linked both to enhanced productivity through nutrient uplift and to losses of coastal
1079 biological communities through offshore advection (Porri et al., 2014; Heye et al., 2022; Jacobs
1080 et al., 2022b). Satellite-derived chlorophyll-a fields show only weak seasonal cycles along the
1081 east coast, reflecting rapid hydrographic variability that can obscure climatological signals
1082 (Lamont et al., 2018). In contrast, targeted in situ observations demonstrated that summer
1083 phytoplankton biomass can exceed winter values during meander-driven upwelling events,
1084 underscoring the limitations of satellite-only interpretations in this region (Russo et al., 2019).

1085

1086 Recent observations have also highlighted emerging biogeochemical concerns along the SAC.
1087 Shelf waters along the Transkei margin have been shown to be undersaturated with respect to
1088 dissolved oxygen, likely reflecting enhanced biological consumption associated with episodic
1089 productivity events (Russo et al., 2019). At larger scales, a modelling study identified a
1090 significant decline in surface dissolved oxygen concentrations within the Agulhas Current over
1091 the past two decades, attributed primarily to warming-induced reductions in oxygen solubility
1092 (Mashifane et al., 2025). Importantly, enhanced cross-frontal mixing during Agulhas meanders
1093 can intermittently increase the influence of Antarctic Intermediate Water along the continental



1094 slope, providing a potential re-oxygenation pathway for bottom shelf waters (Lamont et al.,
1095 2024a).

1096
1097 On the Agulhas Bank itself, sustained research since 2006 has revealed strong coupling between
1098 SAC variability, shelf hydrography, and ecosystem structure. Long-term temperature trends
1099 derived from observations and models indicate both multidecadal warming and episodic cooling
1100 events that have influenced the distribution of commercially important sardine and anchovy
1101 populations (Roy et al., 2007; Rouault et al., 2009; Malan et al., 2019; Lamont et al., 2024b).
1102 Shoreward advection of warm, saline Agulhas waters has been shown to suppress diatom growth
1103 while favouring dinoflagellates, occasionally leading to harmful algal blooms with negative
1104 impacts on fish condition (van der Lingen et al., 2016).

1105
1106 Lagrangian observations and numerical modelling since 2006 have further clarified the role of
1107 the SAC in regulating biological connectivity along the southern African margin. Drifter data
1108 and particle-tracking experiments demonstrated that material entrained into the core of the SAC
1109 is often rapidly advected offshore, reducing nearshore retention of eggs and larvae, while regions
1110 east of Cape Agulhas exhibit comparatively higher retention (Zardi et al., 2011; Lett et al., 2015;
1111 McGrath et al., 2020). Agulhas meanders can transport shelf-derived material tens of kilometres
1112 offshore, influencing population structure and connectivity across the shelf–slope system (Porri
1113 et al., 2014). These findings place the southern Agulhas Current as a dynamic boundary between
1114 retention-dominated and export-dominated regimes. East of Cape Agulhas, circulation supports
1115 larval transport and recruitment on the Agulhas Bank (Lett et al., 2006; Downey-Breedt et al.,
1116 2016; Jacobs et al., 2022b), whereas west of Cape Agulhas the system acts predominantly as a
1117 transport regime, feeding larvae and biota into the Benguela Upwelling System via shelf-edge
1118 jets such as the Benguela Jet (Veitch et al., 2018; Lett et al., 2024).

1119
1120 High-resolution regional modelling studies have played a central role in interpreting these
1121 observations and identifying the mechanisms underlying SAC variability. Models configured
1122 over the Agulhas Bank demonstrate that barotropic and baroclinic instabilities develop as the
1123 current flows over the widened shelf and complex bathymetry, generating meanders, shear-edge
1124 eddies, and filaments that enhance cross-shelf exchange and precondition the retroflection region
1125 (Penven et al., 2006; Loveday et al., 2014; Schubert et al., 2019). More recent simulations
1126 resolving submesoscale dynamics further highlight the importance of fine-scale processes in
1127 shaping SAC structure, variability, and energetics, reinforcing the need for very high-resolution
1128 approaches when assessing shelf interactions and downstream impacts.

1129
1130 In contrast to the relatively constrained Northern Agulhas Current, the Southern Agulhas Current
1131 is characterised by a marked increase in mesoscale variability as the flow interacts with the
1132 widened shelf and complex bathymetry of the Agulhas Bank. This transition fundamentally alters
1133 shelf–slope exchange, downstream circulation, and ecosystem connectivity, and plays a key role
1134 in preconditioning the Agulhas Retroflection.

1135 **3.5. Retroflection and Leakage**

1136 The Agulhas Retroflection, located near the southern tip of Africa, marks the point at which the
1137 Agulhas Current turns sharply back into the Indian Ocean and forms the eastward-flowing
1138 Agulhas Return Current, while intermittently exporting warm, saline Indian Ocean waters into
1139 the South Atlantic via rings, filaments, and other mesoscale structures (Gordon, 1986;
1140 Lutjeharms et al., 1992; Lutjeharms, 2006). This retroflecting configuration is central to Indian–
1141 Atlantic inter-ocean exchange because it governs both the partitioning of transport between the
1142



1143 return flow and the leakage, and the form in which Indian Ocean properties enter the Cape Basin
1144 (Lutjeharms, 2006).

1145
1146 By the mid-1980s, a broad consensus had emerged that the Agulhas Current retroflects almost
1147 completely south of Africa, with most of its transport returning to the Indian Ocean and only a
1148 fraction entering the South Atlantic as Agulhas leakage (Gordon, 1985; Gordon et al., 1987).
1149 Subsequent observational and satellite-based studies demonstrated that this leakage occurs
1150 predominantly through the shedding of large Agulhas rings, which transport substantial volumes
1151 of thermocline and surface waters into the Cape Basin, with smaller contributions from filaments
1152 and intermittent direct exchange (Garzoli and Gordon, 1996; Goñi et al., 1997; Lutjeharms and
1153 Cooper, 1996). Together, these studies established the Agulhas system as a major conduit of heat
1154 and salt between the Indian and Atlantic Oceans.

1155
1156 Despite this qualitative understanding, early quantitative estimates of leakage magnitude
1157 remained highly uncertain. Hydrographic and inverted echo-sounder analyses suggested mean
1158 leakage transports on the order of several Sverdrups, but with strong temporal variability and
1159 substantial methodological dependence (Garzoli and Gordon, 1996). Satellite altimetry further
1160 revealed that individual Agulhas rings carry large heat and salt anomalies into the South Atlantic
1161 (Goñi et al., 1997), reinforcing the climatic significance of leakage events. However, the relative
1162 contributions of rings, filaments, and background flow, as well as the seasonal to interannual
1163 variability of leakage, could not be robustly constrained prior to 2006 because of limited
1164 observational coverage.

1165
1166 By 2006, a coherent conceptual model had emerged in which the retroflection loop undergoes
1167 repeated westward “progradation” events into the South Atlantic, terminating in ring shedding
1168 once the loop extends sufficiently far offshore (Lutjeharms and van Ballegooyen, 1988;
1169 Lutjeharms et al., 1992). These progradation–spawning cycles were inferred to operate on time
1170 scales of weeks, with gradual westward advance followed by abrupt ring detachment
1171 (Lutjeharms and van Ballegooyen, 1988; Lutjeharms, 2006). A key pre-2006 insight was that
1172 upstream variability can modulate ring formation: Natal Pulses reaching the retroflection region
1173 were frequently observed to precipitate ring shedding, although rings could also form in their
1174 absence, indicating a combination of intrinsic instability and upstream triggering (Lutjeharms
1175 and van Ballegooyen, 1988; Lutjeharms, 2006).

1176
1177 Agulhas rings were recognised as exceptionally energetic mesoscale vortices and as the primary
1178 mechanism of property transport into the South Atlantic (Olson and Evans, 1986; Gordon and
1179 Haxby, 1990; Byrne et al., 1995; Lutjeharms, 2006). Pre-2006 estimates of ring-mediated
1180 volume exchange varied widely across observational methods and reference levels, but
1181 commonly yielded values of order 0.5–3 Sv per ring (Olson and Evans, 1986; Gordon and Haxby,
1182 1990; Byrne et al., 1995; Clement and Gordon, 1995), with much smaller contributions attributed
1183 to filaments in the limited cases quantified (Lutjeharms and Cooper, 1996; Lutjeharms, 2006).
1184 As a result, early syntheses emphasised that leakage could not be inferred from ring counts alone,
1185 because property fluxes depend on ring structure, depth penetration, decay pathways, and the
1186 cumulative contribution of non-ring exchange processes (Lutjeharms and Cooper, 1996;
1187 Lutjeharms, 2006).

1188
1189 The downstream fate of Agulhas rings was also an explicit pre-2006 uncertainty. Observational
1190 and modelling evidence indicated that rings can erode or split through interactions with
1191 bathymetric features such as the Erica and Vema seamounts, leading to divergent pathways and
1192 progressive modification of thermohaline properties through air–sea fluxes and ambient mixing



1193 (Byrne et al., 1995; Lutjeharms, 2006). While some rings were observed to persist for several
1194 years, analyses of sea-surface-height anomalies suggested rapid dissipation in the Cape Basin for
1195 a substantial fraction of rings, implying that much of the leaked heat, salt, and vorticity may be
1196 absorbed locally and redistributed by mechanisms other than intact ring translation (Lutjeharms,
1197 2006).

1198

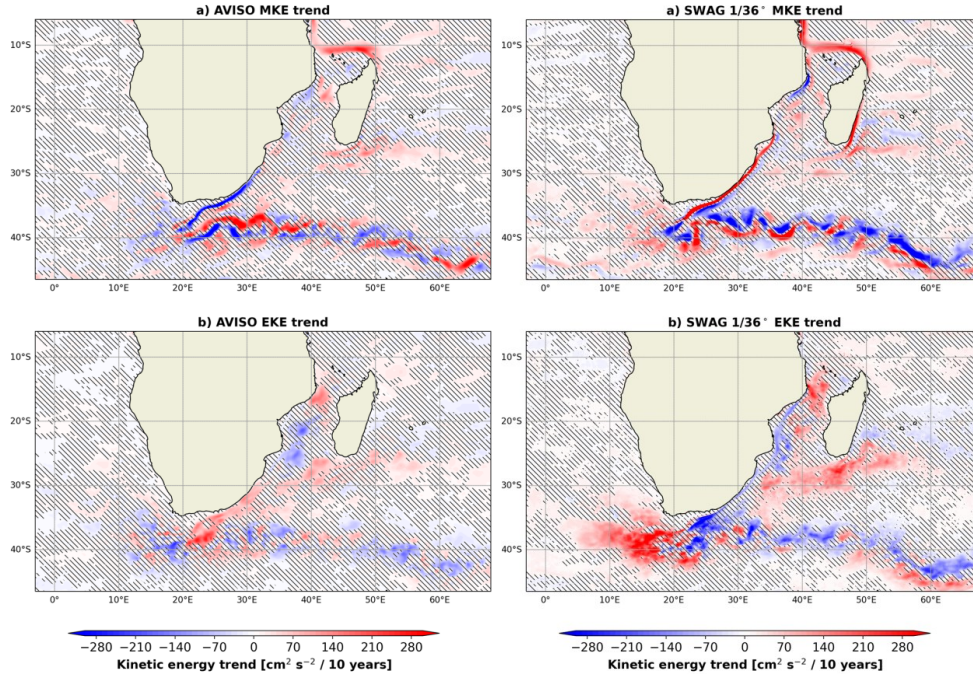
1199 Finally, the retroflection–leakage system was recognised to be embedded within a broader,
1200 highly turbulent Cape Basin environment that includes cyclonic eddies (Cape Basin cyclones)
1201 arising from multiple sources, including Natal Pulse-associated cyclones and lee eddies shed
1202 from the Agulhas Bank (Lutjeharms, 2006). These features were thought to play an important
1203 role in the mixing, redistribution, and transformation of Agulhas waters after leakage, but their
1204 cumulative impact could not be quantified robustly with the observing system available prior to
1205 2006.

1206

1207 Over the past two decades, progress has been driven by (i) longer and more consistent satellite
1208 records, (ii) sustained in situ measurements in key boundary-current and downstream regions,
1209 and (iii) high-resolution modelling capable of resolving the mesoscale and, increasingly,
1210 submesoscale structure that governs exchange. Within this framework, Agulhas leakage is now
1211 routinely treated as the combined export of Indian Ocean waters via rings, filaments, and other
1212 transient features rather than as ring shedding alone (Biastoch et al., 2024; Chelton et al., 2011).

1213

1214 A major focus of post-2006 work has been quantifying Agulhas leakage variability and its
1215 longer-term behaviour, given its relevance to the buoyancy structure of the southeast Atlantic
1216 and potential downstream impacts on the Atlantic Meridional Overturning Circulation (AMOC)
1217 (e.g. Weijer et al., 2002; Speich et al., 2009; Biastoch et al., 2015; Rühs et al., 2022).
1218 Observational analyses revealed that the Agulhas Current system has undergone pronounced
1219 thermodynamic change since the 1980s, with widespread warming of the Agulhas Current, the
1220 retroflection region, and the Agulhas Return Current inferred from satellite and in situ data
1221 (Rouault et al., 2009). This warming was interpreted as a basin-scale signal consistent with
1222 enhanced upper-ocean heat content and stratification, suggesting the potential for altered inter-
1223 ocean exchange. In parallel, satellite altimetry analyses demonstrated a significant intensification
1224 of mesoscale activity across the Greater Agulhas system. Using observations from 1993–2009,
1225 Backeberg et al. (2012) showed robust increases in eddy kinetic energy (EKE) in the
1226 Mozambique Channel, south of Madagascar, along the Agulhas Current pathway, and within the
1227 retroflection region, driven primarily by strengthened trade winds and an intensified South
1228 Equatorial Current.



1229

1230 **Figure 13.** Linear decadal trends in mean kinetic energy (MKE; top panels)
1231 and eddy kinetic energy (EKE; bottom panels) over the period 1993–2018. Trends derived from satellite altimetry
1232 are shown in the left panels, while trends from the 1/36° CROCO regional simulation are shown
1233 in the right panels. Hatched regions indicate areas where trends are not statistically significant at
1234 the 95% confidence level. Adapted from Penven et al. (2025a).

1235

1236 More recently, Penven et al. (2025a) extended this trend analysis using a longer satellite altimetry
1237 record (1993–2018) and an ultra-high-resolution (1/36°) CROCO simulation (SWAG36),
1238 allowing a direct comparison between observed and modelled changes in both mean kinetic
1239 energy (MKE) and EKE (Fig. 13). Their results confirm that the intensification identified by
1240 Backeberg et al. (2012) persists over the extended period, but also reveal pronounced spatial
1241 heterogeneity. These findings imply a dynamical pathway through which increased mesoscale
1242 energy may modulate leakage via changes in ring shedding, filament export, and retroflection
1243 stability, even in the absence of a systematic shift in the mean retroflection position.
1244 Nevertheless, despite these advances, long-term trends in Agulhas leakage remain contested:
1245 some studies report increased leakage since the mid-1960s with enhanced export during the
1246 1990s–2000s (Schwarzkopf et al., 2019), whereas others find no significant long-term trend or
1247 suggest stabilisation since the 1990s (Biastoch et al., 2015; Schmidt et al., 2021). This divergence
1248 highlights the sensitivity of leakage estimates to the diagnostic framework employed (Eulerian
1249 versus Lagrangian), the temporal window considered, and the ability of models to resolve the
1250 nonlinear mesoscale processes governing exchange at the retroflection.

1251

1252 Interactions between leaked Agulhas waters and the Benguela Upwelling System (BUS) have
1253 also been documented as an important cross-system coupling mechanism. Rings and filaments
1254 can enhance offshore export of nutrient- and biota-rich shelf waters into the open ocean
1255 (Duncombe-Rae et al., 1992) and drive episodic shoreward intrusions of warm Agulhas waters
1256 onto the shelf within the BUS (Baker-Yeboah et al., 2010; van der Lingen et al., 2016).



1257 Lagrangian evidence further illustrates the scale of along-margin connectivity: surface drifters
1258 deployed in the KZN Bight have been observed to enter the South Atlantic, with trajectories
1259 ranging from offshore Cape Basin pathways to more shelf-confined routes extending as far north
1260 as Cape Columbine (Guastella and Roberts, 2016). Complementary examples from pollution-
1261 dispersion case studies (e.g., nurdle transport following a Durban harbour spill) similarly
1262 reinforce that the Agulhas system can connect widely separated coastal and shelf environments
1263 along southern Africa on time scales of weeks to months (Schumann et al., 2019).

1264
1265 Beyond physical connectivity, the ecological interpretation of leakage remains actively debated.
1266 Some studies suggest that the episodic nature of leakage can act as a biological barrier that limits
1267 plankton dispersal and contributes to lower diversity in the South Atlantic relative to the South
1268 Indian Ocean (Villar et al., 2015). In contrast, other work demonstrates effective biological
1269 linkage across basins, including inferred connectivity between southern Indian and South
1270 Atlantic rock lobster populations and Lagrangian transport pathways capable of carrying turtle
1271 hatchlings and mangrove propagules into the South Atlantic (Le Gouvello et al., 2020; Silva et
1272 al., 2021; Raw et al., 2023). These apparently divergent perspectives are not mutually exclusive:
1273 they emphasise that leakage can be simultaneously intermittent (limiting continuous dispersal
1274 for some taxa) and, when active, an efficient pathway for episodic long-distance transport.

1275
1276 Overall, research over the past two decades has preserved the core pre-2006 conceptual picture
1277 of a retroflecting current that intermittently sheds rings and filaments, while substantially
1278 sharpening understanding of (i) the multiple pathways and controls on leakage (not ring-only),
1279 (ii) the rapid transformation and mixing of leaked waters within the Cape Basin, and (iii) the
1280 diverse ecological consequences of intermittent inter-ocean exchange. As discussed in Sect 3.3–
1281 3.4, a persistent theme is that upstream and along-path variability—including Natal Pulses and
1282 Southern Agulhas Current instabilities—can modulate the timing and character of retroflection
1283 variability and thus the form and magnitude of Agulhas leakage.

1284
1285 **3.6. Agulhas Return Current**
1286 Prior to 2006, the Agulhas Return Current (ARC) was recognised as the eastward-flowing limb
1287 of the South Indian Ocean subtropical gyre and as the principal pathway by which Agulhas
1288 Current waters return to the Indian Ocean following retroflection south of Africa (Lutjeharms et
1289 al., 1984; Stramma and Lutjeharms, 1997). The ARC was understood to form the dynamical
1290 connection between the South Atlantic Current and the South Indian Ocean Current, flowing
1291 broadly along the Subtropical Convergence and contributing to water-mass exchange between
1292 the two basins (Lutjeharms and Ansorge, 2001).

1293
1294 By the late 1980s and early 1990s, it had become widely accepted that the Agulhas Current
1295 retroflects almost completely south of Africa, such that only a small fraction of its waters enter
1296 the South Atlantic directly. Instead, inter-ocean exchange was recognised to occur primarily
1297 through the shedding of large Agulhas rings and, to a lesser extent, through Agulhas filaments,
1298 while the majority of the Agulhas Current transport feeds the ARC (Gordon, 1985; Gordon et
1299 al., 1987; Lutjeharms and van Ballegooyen, 1988; van Ballegooyen et al., 1994; Lutjeharms and
1300 Cooper, 1996).

1301
1302 Hydrographic sections, surface drifter trajectories, and early satellite altimetry provided the
1303 primary observational basis for describing the structure and pathway of the ARC. These studies
1304 showed a predominantly zonal eastward flow centred near 39–40° S south of Africa, with a
1305 gradual southward displacement downstream, interrupted by substantial meridional excursions
1306 associated with interactions with bottom topography, particularly over major meridional ridges



1307 such as the Agulhas Plateau (Gründlingh, 1978; Daniault and Ménard, 1985; Lutjeharms and van
1308 Ballegooyen, 1984; Lutjeharms and Ansorge, 2001). The region was known to be characterised
1309 by intense mesoscale variability, including recurrent eddy generation and pronounced
1310 meandering of the ARC along the Subtropical Convergence (Cheney et al., 1983; Lutjeharms
1311 and Valentine, 1988).

1312 Quantitative estimates of ARC velocity and transport varied widely among pre-2006 studies.
1313 Geostrophic calculations based on hydrographic sections suggested a marked downstream
1314 decrease in both velocity and volume transport, with values declining from several tens of
1315 Sverdrups near the Agulhas Retroflection to substantially weaker transports farther east
1316 (Gründlingh, 1985; Stramma and Lutjeharms, 1997; Lutjeharms and Ansorge, 2001). Water-
1317 mass analyses demonstrated that temperature and salinity characteristics associated with Agulhas
1318 Current waters could be traced well into the South West Indian Ocean, although the degree of
1319 downstream coherence remained debated (Belkin and Gordon, 1996; Park et al., 1991, 1993).

1320 A key unresolved issue prior to 2006 concerned the eastern termination and downstream
1321 persistence of the ARC. Some studies argued that Agulhas-derived waters remained coherent
1322 beyond 70° E, based on hydrographic and water-mass evidence (Belkin and Gordon, 1996; Park
1323 et al., 1991, 1993), while others suggested substantial branching and dissipation farther west,
1324 implying that the ARC weakened rapidly downstream (Veronis, 1973; Stramma, 1992; Stramma
1325 and Lutjeharms, 1997). As a result, there was no consensus on how far east the ARC remained
1326 a coherent dynamical feature, or on the rate at which its transport diminished along its path.

1327 Although air-sea interaction and mixing processes were recognised as important modifiers of
1328 Agulhas water properties within the ARC—particularly in the vicinity of the retroflection, where
1329 large heat losses and excess evaporation were documented (Mey and Walker, 1990)—the relative
1330 roles of surface forcing, topographic steering, and upstream variability in controlling ARC
1331 structure and variability could not be robustly quantified. This limitation reflected the reliance
1332 on spatially sparse hydrographic snapshots and Lagrangian observations, and the absence of
1333 sustained measurements capable of resolving seasonal to interannual variability along the ARC.

1334 Since 2006, sustained satellite altimetry, improved atmospheric reanalysis products, and eddy-
1335 resolving numerical models have enabled more quantitative assessments of the Agulhas Return
1336 Current (ARC) than were previously possible.

1337 Using satellite altimetry spanning 1993–2020 in combination with ERA5 atmospheric reanalysis
1338 and HYCOM model reanalysis, Lin et al. (2023) presented the most comprehensive analysis to
1339 date of ARC dynamics. Their results demonstrate that the ARC exhibits pronounced spatial
1340 heterogeneity, with distinct dynamical regimes in its western and eastern sectors. The western
1341 ARC (approximately 35–48° E), immediately downstream of the Agulhas Retroflection, is
1342 characterised by elevated eddy kinetic energy (EKE) associated primarily with strong flow-
1343 topography interactions. In contrast, variability in the eastern ARC (approximately 48–70° E) is
1344 more strongly influenced by interactions with the Antarctic Circumpolar Current and large-scale
1345 wind forcing, leading to different modes of variability across the basin.

1346 Lin et al. (2023) report a statistically significant northward migration of the western ARC and a
1347 southward migration of the eastern ARC over the satellite era, resulting in a zonal tilting of the
1348 ARC axis. Such changes could not be robustly assessed prior to 2006 because of insufficient
1349 temporal coverage and observational density.

1350

1351

1352 Lin et al. (2023) report a statistically significant northward migration of the western ARC and a
1353 southward migration of the eastern ARC over the satellite era, resulting in a zonal tilting of the
1354 ARC axis. Such changes could not be robustly assessed prior to 2006 because of insufficient
1355 temporal coverage and observational density.

1356



1357 The dynamical role of ARC meanders in modulating Agulhas Retroflection behaviour is also
1358 better understood. Numerical modelling studies have shown that large-amplitude ARC meanders
1359 and northward excursions can act as precursors to early retroflection events, influencing the
1360 timing and geometry of the Agulhas Current separation from the continental margin. Biastoch et
1361 al. (2008) identified ARC meanders as a key contributor to early retroflection dynamics, while
1362 Johannessen et al. (2020) further demonstrated that the interaction between a large ARC meander
1363 and an inshore cyclonic eddy can promote early retroflection, often in conjunction with upstream
1364 Natal Pulse activity.

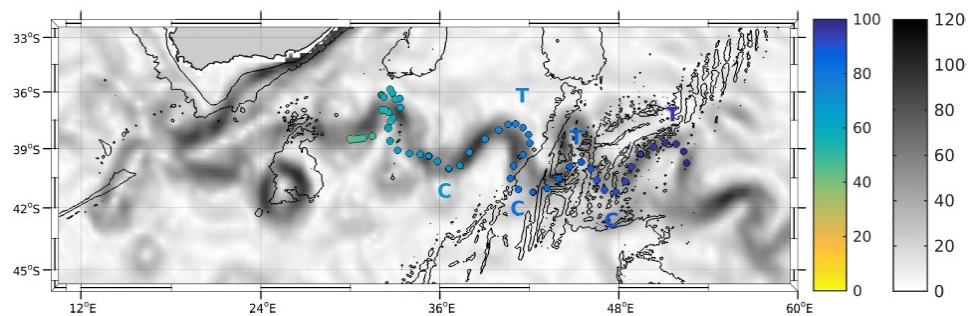
1365

1366 Satellite-based eddy censuses have further documented eddy shedding along the ARC,
1367 complementing earlier observations of mesoscale activity. Analyses of multi-sensor satellite
1368 datasets indicate that mesoscale eddies frequently detach not only in the retroflection region but
1369 also along the ARC pathway, with some eddies subsequently re-merging with the mean flow
1370 while others propagate into the interior of the South West Indian Ocean (Casanova-Masjoan et
1371 al., 2017; Guerra et al., 2018).

1372

1373 Direct in situ observations of the ARC remain limited, but recent targeted measurements have
1374 begun to address this gap. Using data from NOAA Ocean Climate Stations deployed along the
1375 northern boundary of the ARC between November 2010 and March 2011, Braby et al. (2025)
1376 investigated air-sea interaction processes and assessed the performance of satellite-derived and
1377 reanalysis sea surface temperature products. Their analysis (Fig. 14) revealed substantial SST
1378 biases in reanalysis and infrared-only satellite products, particularly under conditions of high
1379 cloud cover, highlighting persistent observational challenges in the ARC region and emphasising
1380 the need for caution when interpreting long-term variability derived solely from remotely sensed
1381 datasets.

1382



1383

1384 **Figure 14.** Position of the air-sea flux moorings on the path of the Agulhas Return Current. Grey
1385 shading indicates the mean geostrophic current speeds in cm s^{-1} over the time of the deployment,
1386 averaged from 30 November 2010 to 8 March 2011. Circles show the position of the mooring
1387 and indicate the number of days since deployment (note that the mooring was stationary until 16
1388 January 2011). Thin black contours show the bathymetry at 200 and 3000 m. Letters "T"
1389 represent the times, after the mooring had broken loose, where the mooring passes through
1390 troughs of Agulhas Return Current meanders, whereas letters "C" represent it passing through
1391 the crests of the current (Adapted by Braby et al., 2025).

1392

3.7. Role in the regional and global climate system

1393 On the basis of its salt and heat fluxes, the Agulhas system was hypothesised to influence the
1394 strength and stability of the Atlantic Meridional Overturning Circulation (AMOC) through salt
1395 compensation of the Atlantic basin. Early numerical modelling studies demonstrated that
1396 variations in Agulhas leakage could modify the salinity of the upper South Atlantic and thereby



1397 affect deep water formation in the North Atlantic (e.g. Weijer et al., 1999). These studies
1398 established a conceptual framework in which increased leakage enhanced AMOC strength, while
1399 reduced leakage weakened it. Importantly, these links were model-based and highly idealised,
1400 and were not supported by direct observational evidence. The sensitivity of the AMOC to
1401 Agulhas leakage was shown to depend strongly on model configuration, background
1402 stratification, and atmospheric forcing, leading to substantial uncertainty in the magnitude and
1403 timescale of the response (Weijer et al., 1999; Biastoch et al., 2003).

1404
1405 In parallel, the Agulhas Current and its extension regions were recognised as sites of
1406 exceptionally strong air-sea heat and moisture fluxes, owing to the large sea-surface temperature
1407 gradients between warm Agulhas waters and the overlying atmosphere. Observational studies
1408 documented mean wintertime heat losses exceeding 200 W m^{-2} in the retroflection region,
1409 indicating intense local coupling between the ocean and atmosphere (Mey and Walker, 1990).
1410 Subsequent analyses suggested that these fluxes could influence regional atmospheric circulation
1411 and storm development south of Africa (Rouault et al., 2003). However, pre-2006 atmospheric
1412 reanalysis products were shown to substantially underestimate latent and sensible heat fluxes
1413 over the Agulhas Current, limiting confidence in climate-scale assessments of air-sea coupling
1414 in this region (Rouault et al., 2003).

1415
1416 Several studies prior to 2006 explored potential links between Agulhas system variability and
1417 regional climate, particularly over southern Africa. Statistical associations were reported
1418 between sea-surface temperature anomalies in the southwest Indian Ocean and summer rainfall
1419 variability over parts of South Africa (Mason, 1990; Walker, 1990; Reason, 2001). More
1420 specifically, relationships were identified between coastal rainfall and the proximity of the
1421 Agulhas Current to the east coast of South Africa (Jury et al., 1993). Atmospheric general
1422 circulation model experiments forced with idealised SST anomalies in the Agulhas system
1423 provided further support for a potential influence on regional rainfall through modifications of
1424 low-level circulation, atmospheric instability, and moisture fluxes (Reason and Mulenga, 1999;
1425 Reason, 2001). Nevertheless, these relationships were largely correlative, and the relative roles
1426 of oceanic forcing versus large-scale atmospheric variability remained unresolved.

1427
1428 A major post-2006 advance has been the improved observational constraint on the transport
1429 variability of the Agulhas Current and its leakage, enabled by sustained mooring arrays and
1430 coordinated observing programmes. The Agulhas Current Time-series (ACT) provided the first
1431 long-term, continuous measurements of Agulhas Current transport, revealing strong variability
1432 on sub-annual to interannual timescales and demonstrating that snapshot hydrographic estimates
1433 substantially underestimate this variability (Beal et al., 2011; Beal et al., 2015). Complementary
1434 observations from the Agulhas System Climate Array (ASCA) and SAMBA further supported
1435 improved estimates of variability in the downstream export of Indian Ocean waters into the South
1436 Atlantic (Eliot and Beal, 2015; McMonigal et al., 2020).

1437
1438 High-resolution modelling studies since 2006 have demonstrated that Agulhas leakage is
1439 sensitive to changes in Southern Hemisphere wind patterns, particularly shifts in the westerlies.
1440 Eddy-resolving simulations showed that poleward intensification and strengthening of westerly
1441 winds enhance leakage by modifying the latitude and stability of the Agulhas Retroflection
1442 (Biastoch et al., 2009; Biastoch and Böning, 2013). Subsequent work extended this framework
1443 by explicitly linking increased leakage to anthropogenic wind trends, suggesting that human-
1444 induced climate change may already be influencing Indo-Atlantic exchange (Biastoch et al.,
1445 2015). More recent synthesis studies have reinforced the view that the Greater Agulhas Current

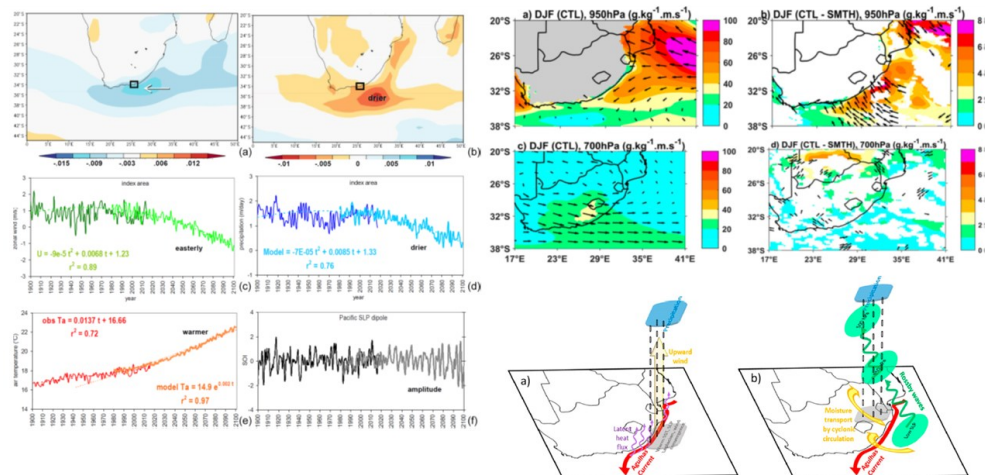


1446 System acts as a dynamically sensitive gateway in the global circulation, capable of responding
 1447 rapidly to basin-scale atmospheric forcing (Beal et al., 2011; Biastoch et al., 2024).

1448
 1449 Post-2006 modelling studies have also continued to support the physical plausibility of a linkage
 1450 between Agulhas leakage variability and the AMOC. Eddy-resolving experiments indicate that
 1451 enhanced leakage increases salinity in the upper South Atlantic, strengthening the upper limb of
 1452 the overturning circulation, while reduced leakage produces the opposite effect (Biastoch et al.,
 1453 2009; Biastoch et al., 2015). Longer integrations suggest that such anomalies can propagate into
 1454 the Atlantic basin on decadal timescales (Biastoch et al., 2024), although direct observational
 1455 confirmation remains lacking.

1456
 1457 At the regional scale, post-2006 advances have substantially clarified the processes by which the
 1458 Agulhas Current system influences weather and climate over southern Africa. High-resolution
 1459 regional atmospheric modelling studies demonstrated that extreme rainfall events along the east
 1460 and south coasts of South Africa are often associated with strong latent heat fluxes from the
 1461 Agulhas Current, low-level jets transporting moisture onshore, and uplift over coastal orography
 1462 (Singleton and Reason, 2006, 2007; Blamey and Reason, 2009). These studies showed that the
 1463 Agulhas system primarily acts to intensify pre-existing weather systems, rather than generating
 1464 rainfall independently.

1465



1466
 1467 **Figure 15.** Climate-scale and regional atmospheric responses associated with the Agulhas
 1468 Current system. Left panels: ECMWF-derived long-term trends (1980–2100, RCP8.5) in (a)
 1469 zonal wind and (b) precipitation, together with time series of area-averaged (c) zonal wind, (d)
 1470 precipitation, and (e) air temperature from ECMWF-20C reanalysis (1900–2010) and ECMWF-
 1471 ESM projections (1980–2100). Panel (f) shows observed and projected Pacific Southern
 1472 Oscillation Index variability; best-fit trends are indicated and time series are annual means
 1473 (adapted from Jury et al., 2020). Upper right panels: Moisture flux from WRF control simulations
 1474 at 950 and 750 hPa, with corresponding moisture flux differences; shading denotes regions
 1475 significant at the 90% level and arrows indicate moisture transport anomalies (adapted from
 1476 Nkwinkwa et al., 2021). Lower panels: Schematic mechanisms linking the Agulhas Current to
 1477 precipitation, illustrating (a) enhanced maritime rainfall over the current due to strong latent heat
 1478 fluxes and low-level convergence, and (b) inland rainfall driven by onshore moisture transport
 1479 and cyclonic circulation, most pronounced in summer but also evident in autumn and spring
 1480 (adapted from Nkwinkwa et al., 2021).



1481

1482 Seasonal-scale regional climate simulations further indicated that the atmospheric response to
1483 the Agulhas system can be interpreted as a quasi-linear response to diabatic heating associated
1484 with warm SSTs in the current, with signatures extending throughout the troposphere (Figure 15;
1485 Njouodo et al., 2018; Imbol Nkwinkwa et al., 2021; Desbiolles et al., 2018). Global and regional
1486 modelling studies also suggested that anomalously warm Agulhas waters can influence the
1487 strength and structure of extratropical cyclones tracking south of Africa, with potential
1488 downstream impacts extending into the southern mid-latitudes (Reason, 2001; Nakamura, 2012).
1489

1490 Air-sea interaction over the Agulhas system was thus reframed as a climate-scale modelling
1491 challenge rather than a purely regional phenomenon. Improved satellite flux products and
1492 reanalysis comparisons revealed that, while representation of surface heat and momentum fluxes
1493 has improved since pre-2006 products, significant biases persist over strong currents and frontal
1494 zones (Rouault et al., 2009). Targeted mooring observations along the Agulhas Return Current
1495 further demonstrated systematic SST biases in reanalysis and infrared-only satellite products
1496 under conditions of high cloud cover, highlighting the sensitivity of regional atmospheric
1497 analyses to accurate representation of the ocean state (Braby et al., 2025).
1498

1499 **4. Summary and conclusions**

1500 This review has synthesised advances in understanding of the Greater Agulhas Current System
1501 (GACS) over the past two decades, motivated in large part by the substantial knowledge gaps
1502 identified by Lutjeharms (2006). At that time, fundamental uncertainties persisted across the
1503 source regions, the Agulhas Current itself, and its downstream outflows, reflecting limitations in
1504 sustained observations, satellite capabilities, and numerical modelling. Since then, significant
1505 progress has been achieved through expanded in situ observing systems, improved satellite
1506 remote sensing, and increasingly high-resolution and physically realistic numerical models.
1507

1508 At the upstream sources of the Agulhas Current, several long-standing questions are now better
1509 understood. In the Mozambique Channel, early debate concerning the existence of a persistent
1510 southward Mozambique Current has been revisited using long-term mooring arrays, satellite
1511 altimetry, and high-resolution modelling. The weight of evidence now supports an eddy-
1512 dominated circulation rather than a continuous boundary current, with both anticyclonic and
1513 cyclonic eddies contributing intermittently to downstream transport. In particular, the existence
1514 and dynamical significance of cyclonic eddies, previously questioned as possible artefacts of
1515 altimetric averaging, have been firmly established. While some ambiguity remains regarding the
1516 presence of weak or intermittent coastal flows under specific conditions, the primary control of
1517 mesoscale eddies on transport through the channel is now well established.
1518

1519 South of Madagascar, one of the most contentious debates identified by Lutjeharms (2006): the
1520 existence of a retroflection of the southern extension of the South East Madagascar Current
1521 (SEMC), has largely been resolved. Subsequent observational and modelling studies have
1522 demonstrated that eastward flow in this region is better attributed to the South Indian Counter
1523 Current (SICC) rather than a persistent SEMC retroflection, effectively closing the so-called
1524 “retro-fiction” debate. However, this resolution has also highlighted the complexity of
1525 circulation south of Madagascar, where multiple currents coexist and interact, and where
1526 connectivity between the SEMC, the Mozambique Channel, and the Agulhas Current is highly
1527 variable and often mediated by mesoscale eddies and dipoles. While understanding of
1528 Madagascar’s role as a dynamical obstacle has improved, particularly through sensitivity



1529 modelling studies, the relative importance of continuous versus intermittent pathways remains
1530 an active area of research.

1531
1532 In the northern Agulhas Current, research over the past two decades has clarified the role of
1533 upstream variability associated with mesoscale eddies originating in the Mozambique Channel
1534 and south of Madagascar, which intermittently feed into and modulate the current. Mooring
1535 arrays, high-resolution Argo float deployments, and satellite altimetry have demonstrated that
1536 variability in transport, lateral position, and intensity of the northern Agulhas Current is strongly
1537 influenced by eddy–current interactions rather than by steady upstream inflow alone. These
1538 studies have largely addressed early uncertainties regarding the degree to which the current is
1539 continuously supplied by its source regions, although quantifying the relative contributions of
1540 different source pathways remains an ongoing challenge.

1541
1542 Knowledge developments in the southern Agulhas Current have centered around resolving
1543 temporal variability, mesoscale structure, and interactions with the continental slope and
1544 atmosphere. Long-term moored observations from the Agulhas Current Time-series (ACT) and
1545 Agulhas System Climate Array (ASCA) have provided unprecedented insight into transport
1546 variability, vertical structure, and the frequency of extreme events such as large meanders and
1547 Natal Pulses. These observations, complemented by satellite-based methods for objectively
1548 tracking the current core and edges, have refined understanding of how variability in the southern
1549 Agulhas Current preconditions the retroflection and influences Agulhas leakage. Despite these
1550 advances, uncertainties remain regarding long-term trends in transport, the response of the
1551 current to changing wind forcing, and the extent to which observed variability reflects natural
1552 versus anthropogenically forced changes, underscoring the continued need for sustained
1553 observations

1554
1555 Downstream of the Agulhas Current, important progress has also been made, though several
1556 questions remain open. The structure and variability of the Agulhas Return Current (ARC) are
1557 now better documented, and its interactions with major bathymetric features, including the
1558 Southwest and Southeast Indian Ridges, the Madagascar Ridge, and the Agulhas Plateau, have
1559 been increasingly explored using observations and models. Nevertheless, uncertainties persist
1560 regarding how ARC waters are transferred back into the subtropical gyre, the extent to which the
1561 ARC recirculates water toward the Agulhas Current, and the mechanisms governing its temporal
1562 variability.

1563
1564 With respect to Agulhas leakage, two decades of research have substantially advanced
1565 understanding of ring shedding, propagation, and decay, as well as the role of leakage in inter-
1566 ocean exchange and its potential influence on the Atlantic Meridional Overturning Circulation.
1567 However, several of the questions posed by Lutjeharms (2006) remain only partially answered.
1568 These include how Agulhas rings of differing size, structure, and vertical extent redistribute heat,
1569 salt, and vorticity in the South Atlantic; the role of atmospheric forcing and convective
1570 overturning in modifying ring evolution; and the sensitivity of leakage magnitude and ring
1571 shedding frequency to changes in wind forcing over the southwest Indian Ocean. Addressing
1572 these questions remains central to understanding the climate relevance of the GACS.

1573
1574 A major development since 2006 has been the identification of several previously unknown
1575 currents. These include the South Indian Counter Current (SICC), now recognised as a multi-
1576 branched eastward flow south of Madagascar; the East Madagascar Undercurrent (EMUC), a
1577 northward-flowing undercurrent beneath the East Madagascar Current; the Southwest
1578 Madagascar Coastal Current (SMACC), a narrow poleward flow along the southern Madagascar

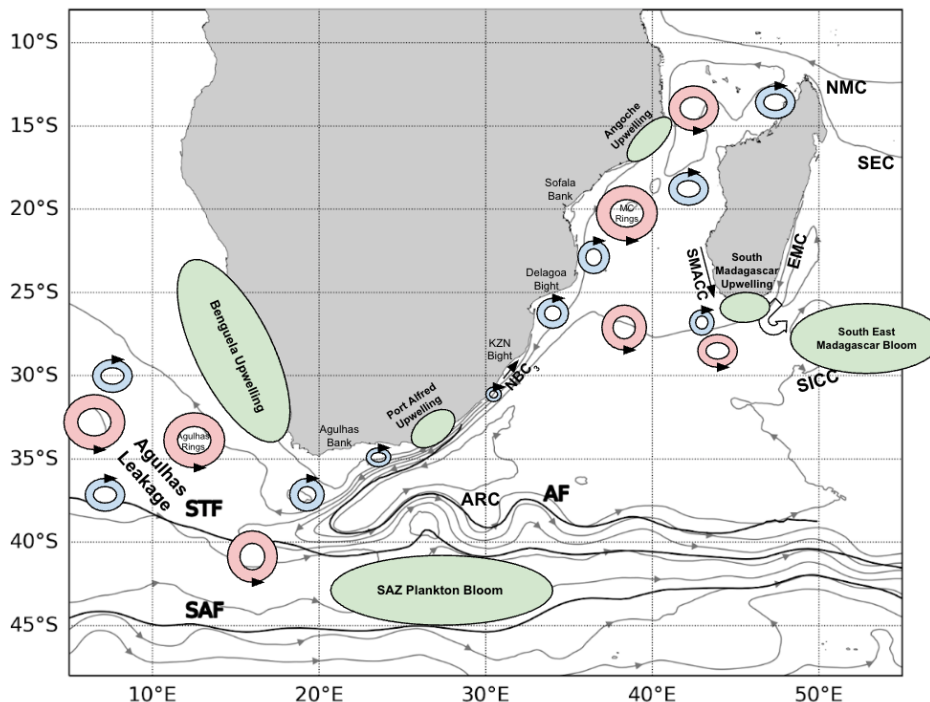


1579 shelf; and the Natal Bright Coastal Counter Current (NBC3), a weak but dynamically significant
1580 northeastward flow along the KwaZulu-Natal shelf. These discoveries have refined our
1581 understanding of circulation pathways, vertical structure, and coastal–open-ocean connectivity
1582 within the GACS, and have highlighted the importance of resolving shelf and undercurrent
1583 processes alongside the major boundary currents.

1584 The advances synthesised in this review are summarised schematically in an updated conceptual
1585 representation of the Greater Agulhas Current System (Fig. 16). The figure integrates
1586 contemporary understanding of the major boundary currents, newly identified currents,
1587 mesoscale and submesoscale features, and key regions of biological productivity, highlighting
1588 both resolved circulation pathways and areas of continued uncertainty. In particular, it reflects
1589 improved knowledge of upstream source regions, eddy-mediated connectivity, the structure and
1590 variability of the Agulhas Current and its downstream extensions, and the spatial coupling
1591 between physical dynamics and ecosystem responses. This updated schematic provides a
1592 consolidated, system-wide view of the GACS as currently understood, and serves as a reference
1593 framework for identifying remaining knowledge gaps and guiding future observational and
1594 modelling efforts.

1595

1596



1597

1598

1599

1600

1601

1602

1603

Figure 16. Updated schematic of the Greater Agulhas Current System, synthesising advances in understanding of circulation pathways, mesoscale and submesoscale features, and regions of enhanced biological activity identified over the past two decades. The schematic highlights major boundary currents, newly identified currents, dominant eddy structures, frontal systems, and key areas of productivity, providing an integrated conceptual overview of the physical and biophysical components of the system.

1604



1605 **4.1. Proposed future directions**

1606 Over the past two decades, inter- and multidisciplinary research within the Greater Agulhas
1607 Current System (GACS) has driven major advances in observational capability, numerical
1608 modelling, and understanding of the system's physical, climatic, and ecological roles. The
1609 integration of satellite remote sensing, long-term mooring arrays, advanced Argo float and glider
1610 technologies, and high-resolution coupled regional models has fundamentally transformed
1611 knowledge of the Agulhas Current and its variability. Large international collaborative
1612 initiatives, including ASCA, ACEP and SAMOC, have addressed many of the key gaps
1613 identified by Lutjeharms (2006), while simultaneously revealing a far greater complexity in the
1614 system's multi-scale dynamics, climate influence, and inter-ocean exchanges than previously
1615 recognised. Despite this progress, substantial challenges and knowledge gaps remain.

1616

1617 A critical priority for future research is the improved observation and representation of
1618 submesoscale and fine-scale processes, which remain poorly resolved by both existing observing
1619 systems and numerical models. These processes are expected to play a central role in vertical
1620 and horizontal mixing, the modulation of Agulhas leakage, and the seasonal to decadal variability
1621 of the system, as well as in associated biogeochemical fluxes. Capturing the transfer of energy
1622 across spatial scales, from submesoscale to mesoscale features such as eddies, meanders, and
1623 Natal Pulses, will require sustained ultra-high-resolution in situ observations combined with
1624 nested and coupled modelling approaches. At present, many dynamically important phenomena,
1625 including Agulhas meanders, Natal Pulses and retroflection shifts, remain sparsely sampled in
1626 situ, with their internal structures largely inferred from models rather than directly observed.

1627

1628 These scientific challenges are compounded by persistent logistical and financial constraints.
1629 Rising operational costs, limited personnel, and intermittent funding have restricted the
1630 continuity of long-term, high-frequency observations, limiting the ability to quantify transient
1631 processes and detect multi-decadal trends. Addressing these limitations will require strategic
1632 investment in modernising and expanding ocean observing infrastructure, including sustained
1633 moored arrays, increased deployment of autonomous platforms such as gliders and
1634 biogeochemical Argo floats, and continued access to satellite missions with improved spatial
1635 resolution and measurement accuracy. Innovative public–private partnerships and cost-effective
1636 approaches, such as integrating sensors onto fishing gear and supporting citizen-science
1637 initiatives, offer promising pathways to enhance coastal observations while increasing societal
1638 engagement and stakeholder value.

1639

1640 Equally important is sustained investment in human capacity development. The growing volume
1641 and complexity of data generated by modern observing systems demand a highly skilled
1642 technical and scientific workforce capable of maintaining instruments, analysing observations,
1643 and integrating data across disciplines. Programmes such as SEAmester provide essential early
1644 exposure to sea-going research and the Agulhas system, but must be complemented by long-term
1645 training, mentorship, and career development pathways. Strengthening technical and scientific
1646 expertise is particularly critical in the context of climate change, increasing resource pressures,
1647 and highly competitive funding environments, where advanced infrastructure alone is
1648 insufficient without the capacity to fully exploit it.

1649

1650 Finally, the future trajectory of Agulhas Current research will depend on coordinated governance
1651 and sustained commitment from national, regional, and international stakeholders. Recognising
1652 the Agulhas Current system as a strategic natural asset, central to climate regulation, ecosystem
1653 productivity, and global overturning circulation, should underpin stable funding for long-term
1654 observations, acquisition of state-of-the-art technology, and retention of skilled personnel. The



1655 next two decades represent a pivotal opportunity: with adequate investment, integrated observing
1656 and modelling frameworks, and a well-trained interdisciplinary workforce, South Africa is
1657 uniquely positioned to lead globally in Agulhas Current research. Failure to capitalise on this
1658 opportunity risks not only scientific setbacks, but also weakened climate adaptation and
1659 conservation efforts in an increasingly coupled ocean–climate–ecosystem system.

1660

1661 **References**

1662 Backeberg, B. C., Bertino, L., Johannessen, J. A.: Evaluating two numerical advection schemes
1663 in HYCOM for eddy-resolving modelling of the Agulhas Current. *Ocean Sci.* 5, 173–190,
1664 2009.

1665 Backeberg, B. C., and C. J. C. Reason (2010), A connection between the South Equatorial
1666 Current north of Madagascar and Mozambique Channel Eddies, *Geophys. Res. Lett.*, 37,
1667 L04604, doi:10.1029/2009GL041950.

1668 Backeberg, B. C., Penven, P., and Rouault, M.: Impact of intensified Indian Ocean winds on the
1669 mesoscale variability of the Agulhas system. *Nat Climate Change*, 2, 608–612, 2012.

1670 Baker-Yeboah, S., Byrne, D.A., and Watts, D.R.: Observations of mesoscale eddies in the South
1671 Atlantic Cape Basin: Baroclinic and deep barotropic eddy variability, *J. Geophys. Res.*,
1672 115, C12069, https://doi.org/10.1029/2010JC006236, 2010.

1673 Barlow, R., Kyewalyanga, M., Sessions, H., van den Berg, M., and Morris, T.: Phytoplankton
1674 pigments, functional types, and absorption properties in the Delagoa and Natal Bights of
1675 the Agulhas ecosystem, *Estuar. Coast. Shelf Sci.*, 80, 201–211,
1676 https://doi.org/10.1016/j.ecss.2008.07.022, 2008.

1677 Barlow, R., Lamont, T., Morris, T., Sessions, H., and van den Berg, M.: Adaptation of
1678 phytoplankton communities to mesoscale eddies in the Mozambique Channel. *Deep-Sea*
1679 *Res. II*, 100, 106–118, http://dx.doi.org/10.1016/j.dsr2.2013.10.020, 2014.

1680 Barnier, B., Madec, G., Penduff, T., Molines, J.-M., Treguier, A.-M., Le Sommer, J., Beckmann,
1681 A., Biastoch, A., Böning, C., Dengg, J., Derval, C., Durand, E., Gulev, S., Remy, E.,
1682 Talandier, C., Theetten, S., Maltrud, M., McClean, J., Cuevas, B. D.: Impact of partial
1683 steps and momentum advection schemes in a global ocean circulation model at eddy-
1684 permitting resolution. *Ocean Dyn.* 56, 543–567, doi:10.1007/s10236-006-0082-1, 2006.

1685 Beal, L., De Ruijter, W., Biastoch, A. et al.: On the role of the Agulhas system in ocean
1686 circulation and climate. *Nature* 472, 429–436, https://doi.org/10.1038/nature09983, 2011.

1687 Beal, L.M., and Bryden, H.L.: Observations of an Agulhas Undercurrent, *Deep-Sea Res. I*, 44,
1688 1715–1724, https://doi.org/10.1016/S0967-0637(97)00033-2, 1997.

1689 Beal, L.M., Chereskin, T.K., Lenn, Y.D., and Eliot, S.: The sources and mixing characteristics
1690 of the Agulhas Current. *J. Phys. Oceanogr.*, 36, 2060–2074.
1691 https://doi.org/10.1175/JPO2964.1, 2006.

1692 Beal, L.M., de Ruijter, W.P.M., Biastoch, A., Zahn, R., and SCOR/WCRP/IAPSO Working
1693 Group 136,: On the role of the Agulhas system in ocean circulation and climate, *Nature*,
1694 472, 429–436, https://doi.org/10.1038/nature09983, 2011.

1695 Beal, L.M., Eliot, S., Houk, A., and Leber, G.M.: Capturing the transport variability of a
1696 Western Boundary Jet: Results from the Agulhas Current Time-Series Experiment (ACT),
1697 *J. Phys. Oceanogr.*, 45, 1302–1324, https://doi.org/10.1175/JPO-D-14-0119.1, 2015.

1698 Beal, L.M.: A time series of Agulhas Undercurrent transport, *J. Phys. Oceanogr.*, 39, 2436–2450,
1699 https://doi.org/10.1175/2009JPO4195.1, 2009.

1700 Beech N., Rackow, T., Wang, Q., Jung, T.: Long-term evolution of ocean eddy activity in a
1701 warming world, *Nat Clim. Change*, 12, 910–917, 2022.

1702 Biastoch, A., and Böning, C.W.: Anthropogenic impact on Agulhas leakage. *Geophys. Res.*
1703 *Lett.*, 40, 1138–1143, https://doi.org/10.1002/grl.50243, 2013.



1704 Biastoch, A., and Krauss, W.: The role of mesoscale eddies in the source regions of the Agulhas
1705 Current, *J. Phys. Oceanogr.*, 29, 2303–2317, [https://doi.org/10.1175/1520-0485\(1999\)0292303:TROMEI-2.0.CO;2](https://doi.org/10.1175/1520-0485(1999)0292303:TROMEI-2.0.CO;2), 1999.

1706 Biastoch, A., Böning, C. W., Lutjeharms, J. R. E.: Agulhas leakage dynamics affects decadal
1707 variability in atlantic overturning circulation. *Nature* 456, 489-492, 2008a.

1708 Biastoch, A., Böning, C.W., Schwarzkopf, F.U., and Lutjeharms, J.R.E.: Increase in Agulhas
1709 leakage due to poleward shift of Southern Hemisphere westerlies, *Nature*, 462, 495–498,
1710 <https://doi.org/10.1038/nature08519>, 2009.

1711 Biastoch, A., Durgadoo, J.V., Morrison, A.K., van Sebille, E., Weijer, W., and Griffies, S.M.:
1712 Atlantic multi-decadal oscillation covaries with Agulhas leakage, *Nat. Commun.*, 6, 10082,
1713 <https://doi.org/10.1038/ncomms10082>, 2015.

1714 Biastoch, A., Lutjeharms, J.R.E., Böning, C.W., and Scheinert, M.: Mesoscale perturbations
1715 control inter-ocean exchange south of Africa, *Geophys. Res. Lett.*, 35, L20602,
1716 <https://doi.org/10.1029/2008GL035132>, 2008b.

1717 Biastoch, A., Rühs, S., Ivanciu, I., Schwarzkopf, F.U., Veitch, J., Reason, C., Zorita, E., Tim,
1718 N., Hünicke, B., Vafeidis, A.T., Santamaría-Aguilar, S., Kupfer, S., and Soltau, F.: The
1719 Agulhas Current System as an important driver for oceanic and terrestrial climate, in:
1720 Sustainability of Southern African ecosystems under global change, edited by: von Maltitz,
1721 G.P., Midgley, G.F., Veitch, J., Brümmer, C., Rötter, R.P., Viehberg, F.A., and Veste M.,
1722 Springer Cham, 191–220, https://doi.org/10.1007/978-3-031-10948-5_8, 2024.

1723 Blamey, R.C., and Reason, C.J.C.: Numerical simulation of a mesoscale convective system over
1724 the east coast of South Africa, *Tellus A: Dyn. Meteorol. Oceanogr.*, 61, 17–34,
1725 <https://doi.org/10.1111/j.1600-0870.2007.00366.x>, 2009.

1726 Boebel, O., Lutjeharms, J., Schmid C., Zenk, W., Rossby, T., and Barron, C.: The Cape
1727 Cauldron: a regime of turbulent inter-ocean exchange, *Deep-Sea Res. II*, 50, 57–86,
1728 [https://doi.org/10.1016/S0967-0645\(02\)00379-X](https://doi.org/10.1016/S0967-0645(02)00379-X), 2003.

1729 Boudra, D., Chassignet, E. P.: Dynamics of the Agulhas retroflection and ring formation in a
1730 numerical model. Part I: The vorticity balance. *J. Phys. Oceanogr.* 18, 280-303, 1988.

1731 Boyd, A.J., and Shillington, F.A.: Physical forcing and circulation patterns on the Agulhas Bank,
1732 S. Afr. J. Sci., 90, 114–122, https://hdl.handle.net/10520/AJA00382353_4624, 1994.

1733 Braby, L., Backeberg, B. C., Ansorge, I., Roberts, M.J., Krug, M., Reason, C. J. C.: Observed
1734 eddy dissipation in the Agulhas Current, *Geophys. Res. Lett.*, 43, 8143–8150,
1735 [doi:10.1002/2016GL069480](https://doi.org/10.1002/2016GL069480), 2016.

1736 Braby, L., Cronin, M. F., Krug, M., Swart, S., Hermes, J. C.: Challenges resolving the warm
1737 Agulhas Return Current extension lead to biases in satellite and reanalysis products, *QJR
1738 Meteorol Soc.* 2025;151:e4947. <https://doi.org/10.1002/qj.4947>, 2025.

1739 Casal, T.G.D., Beal., L.M., Lumpkin, R., and Johns, W.E.: Structure and downstream evolution
1740 of the Agulhas Current system during a quasi-synoptic survey in February–March 2003, *J.
1741 Geophys. Res. Oceans*, 114, C03001, <https://doi.org/10.1029/2008JC004954>, 2009.

1742 Chapman, P., Di Marco, S.F., Davis, R.E., and Coward, A.C.: Flow at intermediate depths
1743 around Madagascar based on ALACE float trajectories, *Deep-Sea Res. II*, 50, 1957–1986,
1744 [https://doi.org/10.1016/S0967-0645\(03\)00040-7](https://doi.org/10.1016/S0967-0645(03)00040-7), 2003.

1745 Chenillat, F., E. Deshaies, A. Arens, P. Penven. : Role of mesoscale eddies in the
1746 biogeochemistry of the Mozambique Channel, *Front. Mar. Sci.*, 11, 1402776, 2024.

1747 Chevane, C. M., P. Penven, F. P. J. Nehama and C. J. C. Reason.: Modelling the tides and their
1748 impacts on the vertical stratification over the Sofala Bank, Mozambique, *Afr. J. Mar. Sci.*,
1749 38, 465-479, 2016.

1750



1752 Cossa, O., Pous, S., Penven, P., Capet, X., and Reason, C.J.C.: Modelling cyclonic eddies in the
1753 Delagoa Bight region, *Cont. Shelf Res.*, 119, 14–29,
1754 <http://dx.doi.org/10.1016/j.csr.2016.03.006>, 2016.

1755 Daher, H., Beal, L.M., and Scharzkopf, F.U.: A new improved estimation of Agulhas leakage
1756 using observations and simulations of lagrangian floats and drifters, *J. Geophys. Res. Oceans*, 125, e2019JC015753, <https://doi.org/10.1029/2019JC015753>, 2020.

1757 de Ruijter, W. P. M., Biastoch, A., Drijfhout, S. S., Lutjeharms, J. R. E., Matano, R. P., Pichevin,
1758 T., van Leeuwen, P. J., and Weijer, W.: Indian-Atlantic interocean exchange: Dynamics,
1759 estimation and impact. *J. Geophys. Res.*, 104, 20885–20910, 1999.

1760 de Ruijter, W.P.M., Ridderinkhof, H., Lutjeharms, J.R.E., Schouten, M.W., and Veth, C.:
1761 Observations of the flow in the Mozambique Channel, *Geophys. Res. Lett.*, 29, 1401–
1762 1403, <https://doi.org/10.1029/2001GL013714>, 2002.

1763 de Ruijter, W.P.M., van Aken, H.M., Beier, E.J., Lutjeharms, J.R.E., Matano, R.P., and
1764 Schouten, M.W.: Eddies and dipoles around South Madagascar: formation, pathways and
1765 large-scale impact, *Deep-Sea Res. I*, 51, 383–400,
1766 <https://doi.org/10.1016/j.dsr.2003.10.011>, 2004.

1767 Donohue, K.A., Firing, E., and Beal, L.M.: Comparison of three velocity section of the Agulhas
1768 Current and Agulhas Undercurrent, *J. Geophys. Res.*, 105, 28585–28593,

1769 Downey-Breedt, N.J., Roberts, M.J., Sauer, W.H.H., and Chang, N.: Modelling transport of
1770 inshore and deep-spawned chokka squid (*Loligo reynaudii*) paralarvae off South Africa: the
1771 potential contribution of deep spawning to recruitment, *Fish. Oceanogr.*, 25, 28–43,
1772 <https://doi.org/10.1111/fog.12132>, 2015.

1773 Durgadoo, J.V., Loveday, B., Reason, C., Penven, P., and Biastoch, A.: Agulhas leakage
1774 predominantly responds to the southern hemisphere westerlies, *J. Phys. Oceanogr.*, 43,
1775 2113–2131, <https://doi.org/10.1175/JPO-D-13-047.1>, 2013.

1776 Elipot, S., and Beal, L.M.: Characteristics, energetics, and origins of Agulhas Current meanders
1777 and their limited influence on ring shedding, *J. Phys. Oceanogr.*, 45, 2294–2314,
1778 <https://doi.org/10.1175/JPO-D-14-0254.1>, 2015.

1779 Gill, A.E., and Schumann, E.H.: Topographically induced changes in the structure of an inertial
1780 coastal jet: Application to the Agulhas Current, *J. Phys. Oceanogr.*, 9, 975–991,
1781 [https://doi.org/10.1175/1520-0485\(1979\)009<0975:TICITS>2.0.CO;2](https://doi.org/10.1175/1520-0485(1979)009<0975:TICITS>2.0.CO;2), 1979.

1782 Gordon, A.L.: The brawnietest retroflection, *Nature*, 421, 904–905,
1783 <https://doi.org/10.1038/421904a>, 2003.

1784 Goschen, W.S., Bornman, T.G., Deyzel, S.H.P., and Schumann, E.H.: Coastal upwelling on the
1785 far eastern Agulhas Bank associated with large meanders in the Agulhas Current, *Cont. Shelf Res.*,
1786 101, 34–46, <https://doi.org/10.1016/j.csr.2015.04.004>, 2015.

1787 Granger, R., Smart, S. M., Foreman, A., Auderset, A., Campbell, E. C., Marshall, T. A., et al.:
1788 Tracking Agulhas leakage in the South Atlantic Using Modern Planktic Foraminifera
1789 Nitrogen Isotopes. *Geoch. Geophys. Geosys.*, 25(9),
1790 <https://doi.org/10.1029/2023GC011190>, 2024

1791 Großelindemann, H., Castruccio, F.S., Danabasoglu, G., and Biastoch A.: Long-term variability
1792 and trends in the Agulhas leakage and its impacts on the global overturning, *Ocean Sci.*,
1793 21, 93–112, <https://doi.org/10.5194/os-21-93-2025>, 2025.

1794 Guastella, L.M., and Roberts, M.J.: 2016. Dynamics and role of the Durban cyclonic eddy in the
1795 KwaZulu-Natal Bight ecosystem, *Afr. J. Mar. Sci.*, 38, S23–S42,
1796 <https://doi.org/10.2989/1814232X.2016.1159982>, 2016.

1797 Halo, I., Backeberg, B., Penven, P., Ansorge, I., Reason, C., and Ullgren, J.E.: Eddy properties
1798 in the Mozambique Channel: A comparison between observations and two numerical
1799 ocean circulation models. *Deep-Sea Res. II*, 100, 38–53,
1800 <http://dx.doi.org/10.1016/j.dsr2.2013.10.015>, 2014.

1801



1802 Halo, I., Penven, P., Backeberg, B., Ansorge, I., Shillington, F., and Roman, R.: Mesoscale eddy
1803 variability in the southern extension of the East Madagascar Current: Seasonal cycle,
1804 energy conversion terms, and eddy mean properties, *J. Geophys. Res.*, 119,
1805 2014JC009820, 2014b.

1806 Hart-Davis, M.G., Backeberg, B.C., Halo, I., van Sebille, E. and Johannessen, J.A.: Assessing
1807 the accuracy of satellite derived ocean currents by comparing observed and virtual buoys
1808 in the Greater Agulhas Region. *Remote Sensing of Environment*, 216, pp.735-746.
1809 <https://doi.org/10.1016/j.rse.2018.03.040>, 2018.

1810 Heye, S., Krug, M., Penven, P., Hart-Davis, M.: The Natal Bight Coastal Counter-Current: a
1811 modelling study, *Cont. Shelf Res.*, 249, 104852,
1812 <https://doi.org/10.1016/j.csr.2022.104852>, 2022.

1813 Huang, Y., Nicholson, D., Huang, B., & Cassar, N.: Global Estimates of Marine Gross Primary
1814 Production Based on Machine Learning Upscaling of Field Observations. *Glob Biogeoch*
1815 *Cycl*, 35(3). <https://doi.org/10.1029/2020GB006718>, 2021.

1816 Imbol Nkwinkwa, A.S.N., Rouault, M., Keenlyside, N., and Koseki, S.: Impact of the Agulhas
1817 Current on Southern Africa precipitation: A modelling study, *J. Climate*, 34m 9973–9988,
1818 <https://doi.org/10.1175/JCLI-D-20-0627.1>, 2021.

1819 Imbol, Arielle Stela, Mathieu Rouault, Johnny A. Johannessen (2019), Latent heat flux in the
1820 Agulhas Current, *Remote Sensing*, 2019, 11, 1576; doi:10.3390/rs11131576.

1821 Jackson, J.M., Rainville, L., Roberts, M.J., McQuaid, C.D., and Lutjeharms, J.R.E.: Mesoscale
1822 bio-physical interactions between the Agulhas Current and the Agulhas Bank, South
1823 Africa, *Cont. Shelf Res.*, 49, 10–24, <https://doi.org/10.1016/j.csr.2012.09.005>, 2012.

1824 Jacobs, Z., Kelly, S., Jebri, F., Roberts, M., Srokosz, M., Sauer, W., Hancke, L., and Popova, E.:
1825 Retention properties of the Agulhas bank and their relevance to the chokka squid life cycle,
1826 *Deep-Sea Res. II*, 202, 105151, <https://doi.org/10.1016/j.dsr2.2022.105151>, 2022b.

1827 Jacobs, Z., Roberts, M., Jebri, F., Srokosz, M., Kelly, S., Sauer, W., Bruggeman, J., and Popova, E.:
1828 Drivers of productivity on the Agulhas Bank and the importance for marine ecosystems,
1829 *Deep-Sea Res. II*, 199, 105080, <https://doi.org/10.1016/j.dsr2.2022.105080>, 2022a.

1830 Johannessen, J.A., B. Chapron, F. Collard, V. Kudryavtsev, A. Mouché, D. Akimov, and K.-F.
1831 Dagestad (2008), Direct ocean surface velocity measurements from Space: Improved
1832 quantitative interpretation of Envisat ASAR observations, *Geophys Res Lett*, 28
1833 November, 2008.

1834 Johannessen, J.A., T. Lamont, C. Russo, Roshin P. Raj, F. Collard and B. Chapron.: Using
1835 advanced visualization tool to study the dynamics of the Agulhas Current: The Early
1836 retroflection. In *Proceedings of the Nansen-Tutu Center 10-years Anniversary*
1837 *Symposium*, Cape Town, South Africa, 10-12 March 2020.

1838 Johannessen, Johnny A., Bertrand Chapron, Fabrice Collard, Bjørn Backeberg (2014), Use of
1839 SAR data to monitor the Greater Agulhas Current, In *Remote Sensing of the African Seas*
1840 edited by V. Barale and M. Gade, ISBN 978-94-017-8007-0, Springer, 2014.

1841 Johnson, J.: Investigating Agulhas Early Retroflections and Ocean Dynamics: SWOT vs.
1842 Conventional Altimetry. Master's Thesis Technical Universtiyy of Munich.
1843 <https://mediatum.ub.tum.de/1772673>, 2025.

1844 José, Y., Penven, P., Aumont, O., Machu, E., Moloney, C., Shillington, F., and Maury, O.:
1845 Suppressing and enhancing effects of mesoscale dynamics on biological production in the
1846 Mozambique Channel, *J. Mar. Sys.*, 158, 129-139, 2016.

1847 José, Y.S., Aumont, O., Machu, E., Penven, P., Moloney, C.L and Maury, O.: Influence of
1848 mesoscale eddies on biological production in the Mozambique Channel: Several contrasted
1849 examples from a coupled ocean- biogeochemistry model, *Deep-Sea Res. II*, 100, 79-93,
1850 2014.



1851 Jury, M.R., Valentine, H.R., and Lutjeharms, J.R.E.: Influence of the Agulhas Current on
1852 summer rainfall along the southeast coast of South Africa, *J. App. Meteorol. Clim.*, 32,
1853 1282–1287, [https://doi.org/10.1175/1520-0450\(1993\)032<1282:IOTACO>2.0.CO;2](https://doi.org/10.1175/1520-0450(1993)032<1282:IOTACO>2.0.CO;2),
1854 1993.

1855 Jury, M. R.: Marine climate change over the eastern Agulhas Bank of South Africa, *Ocean Sci.*,
1856 16, 1529–1544, <https://doi.org/10.5194/os-16-1529-2020>, 2020.

1857 Krug, M., and Penven, P.: New perspectives on Natal Pulses from satellite observations, *J.
1858 Geophys. Res. Oceans*, 116, C07013, <https://doi.org/10.1029/2010JC006866>, 2011.

1859 Krug, M., and Tournadre, J.: Satellite observations of an annual cycle in the Agulhas Current,
1860 *Geophys. Res. Lett.*, 39, L15607, <https://doi.org/10.1029/2012GL052335>, 2012.

1861 Krug, M., Collard, A.M.F., Johannessen, J.A., and Chapron, B.: Mapping the Agulhas Current
1862 from space: An assessment of ASAR surface current velocities, *J. Geophys. Res. Oceans*,
1863 115, C10026, <https://doi.org/10.1029/2009JC006050>, 2010.

1864 Krug, M., D. Schilperoort, F. Collard, M.W. Hansen, M. Rouault; Signature of the Agulhas
1865 Current in high resolution satellite derived wind fields, *Remote Sensing of Environment*,
1866 Vol. 217, Nov. 2018, Pages 340–351.Krug, M., Swart, S., and Gula, J.: Submesoscale
1867 cyclones in the Agulhas Current, *Geophys. Res. Lett.*, 44, 346–354,
1868 <https://doi.org/10.1002/2016GL071006>, 2017.

1869 Krug, M., Tournadre, J., and Dufois, F.: Interactions between the Agulhas Current and the
1870 eastern margin of the Agulhas Bank, *Cont. Shelf Res.*, 81, 67–79,
1871 <https://doi.org/10.1016/j.csr.2014.02.020>, 2014.

1872 Kyewalyanga, M.S., Naik, R., Hedge, S., Raman, M., Barlow, R., and Roberts, M.:
1873 Phytoplankton biomass and primary production in Delagoa Bight Mozambique:
1874 Application of remote sensing, *Estuar. Coast. Shelf Sci.*, 74, 429–436,
1875 <https://doi.org/10.1016/j.ecss.2007.04.027>, 2007.

1876 Lamont, T., and Barlow, R.G.: Environmental influence on phytoplankton production during
1877 summer on the KwaZulu-Natal shelf of the Agulhas ecosystem, *Afr. J. Mar. Sci.*, 37, 485–
1878 501, <https://doi.org/10.2989/1814232X.2015.1108228>, 2015.

1879 Lamont, T., Barlow, R.G., Morris, T., and van den Berg, M.A.: Characterisation of mesoscale
1880 features and phytoplankton variability in the Mozambique Channel. *Deep-Sea Res. II*,
1881 100, 94–105, <http://dx.doi.org/10.1016/j.dsr2.2013.10.019>, 2014.

1882 Lamont, T., Brewin, R.J.W., and Barlow, R.G.: Seasonal variation in remotely-sensed
1883 phytoplankton size structure around southern Africa, *Remote Sens. Environ.*, 204, 617–
1884 631, <https://doi.org/10.1016/j.rse.2017.09.038>, 2018.

1885 Lamont, T., Halo, I., and Russo, C.S.: Impacts of Agulhas Current meanders on intermediate
1886 water masses along the adjacent continental slope and shelf, *Cont. Shelf Res.*, 274, 105197,
1887 <https://doi.org/10.1016/j.csr.2024.105197>, 2024a.

1888 Lamont, T., Roberts, M.J., Barlow, R.G., Morris, T., and van den Berg, M.A., Circulation
1889 patterns in the Delagoa Bight, Mozambique, and the influence of deep ocean eddies. *Afr.
1890 J. Mar. Sci.*, 32, 553–562, <https://doi.org/10.2989/1814232X.2010.538147>, 2010.

1891 Lamont, T., van den Berg, M.A., and Barlow, R.G.: Agulhas Current Influence on the shelf
1892 dynamics of the KwaZulu-Natal Bight, *J. Phys. Oceanogr.*, 46, 1323–1338,
1893 <https://doi.org/10.1175/JPO-D-15-0152.1>, 2016.

1894 Le Gouvello, D.Z.M., Hart-Davis, M.G., Backberg, B.C., and Nel, R.: Effects of swimming
1895 behaviour and oceanography on sea turtle hatchling dispersal at the intersection of two
1896 ocean current systems, *Ecol. Model.*, 431, 109130,
1897 <https://doi.org/10.1016/j.ecolmodel.2020.109130>, 2020.

1898 Lett, C., Malauene, B.S., Hoareau, T.B., Kaplan, D.M., and Porri, F.: Corridors and barriers to
1899 marine connectivity around southern Africa, *Mar. Ecol. Prog. Ser.*, 731, 105–127,
1900 <https://doi.org/10.3354/meps14312>, 2024.



1901 Lett, C., Roy, C., Levasseur, A., van der Lingen, C.D., and Mullon, C.: Simulation and
1902 quantification of enrichment and retention processes in the southern Benguela, Fish.
1903 Oceanogr., 15, 363–372, <https://doi.org/10.1111/j.1365-2419.2005.00392.x>, 2006.

1904 Lett, C., van der Lingen, C.D., Loveday, B.R., and Moloney, C.L.: Biophysical models of larval
1905 dispersal in the Benguela Current ecosystem, Afr. J. Mar. Sci., 37, 457–465,
1906 <http://dx.doi.org/10.2989/1814232X.2015.1105295>, 2015.

1907 Lin, Y., Lin, L., Wang, D., Yang, X.-Y.: Inclination Trend of the Agulhas Return Current Path
1908 in Three Decades. Remote Sens., 15, 5652. <https://doi.org/10.3390/rs15245652>, 2023.

1909 Loveday, B.R., Durgadoo, J.V., Reason, C.J.C., Biastoch, A., and Penven, P.: Decoupling of the
1910 Agulhas leakage from the Agulhas Current, J. Phys. Oceanogr., 44, 1776–1797,
1911 <https://doi.org/10.1175/JPO-D-13-093.1>, 2014.

1912 Lutjeharms, J. R. E., Webb, D. J.: Modelling the Agulhas current system with FRAM (Fine
1913 Resolution Antarctic Model). Deep Sea Res., Part I, 42, 523–551, 1995.

1914 Lutjeharms, J.R.E., Biastoch, A., van der Werf, P.M., de Ruijter, W.P.M., and Ridderinkhof, H.:
1915 On the discontinuous nature of the Mozambique Current: research letter, S. Afr. J. Sci.,
1916 108, #428, <https://doi.org/10.4102/sajs.v108i1/2.428>, 2012.

1917 Lutjeharms, J.R.E., Durgadoo, J.V., Schapira, M., and McQuaid, C.D.: First oceanographic
1918 survey of the entire continental shelf adjacent to the northern Agulhas Current: news &
1919 views, S. Afr. J. Marine Sci., 106, #410, <https://hdl.handle.net/10520/EJC97083>, 2010.

1920 Lutjeharms, J.R.E., Gründlingh, M.L., and Carter, R.A.: Topographically induced upwelling in
1921 the Natal Bight. S Afr J Sci., 85, 310–316, 1989.

1922 Lutjeharms, J.R.E., Penven, P., and Roy, C.: Modelling the shear edge eddies of the southern
1923 Agulhas Current, Cont. Shelf Res., 23, 1099–1115, [https://doi.org/10.1016/S0278-4343\(03\)00106-7](https://doi.org/10.1016/S0278-4343(03)00106-7), 2003.

1925 Lutjeharms, J.R.E.: The Agulhas Current, Springer, Berlin, <https://doi.org/10.1007/3-540-37212-1>, 2006.

1927 Lutjeharms JRE, Bornman TG.: The importance of the greater Agulhas Current is increasingly
1928 being recognised. S Afr J Sci.106(3/4), Art. #160,. DOI: 10.4102/sajs. v106i3/4.160, 2010.

1929 Malan, B., Durgadoo, J.V., Biastoch, A., Reason, C., and Hermes, J: Multidecadal wind
1930 variability drives temperature shifts on the Agulhas Bank, J. Geophys. Res. Oceans, 124,
1931 3021–3035. <https://doi.org/10.1029/2018JC014614>, 2019.

1932 Malan, N., Backeberg, B., Biastoch, A., Durgadoo, J.V., Samuelson, A., Reason, C., and
1933 Hermes, J.: Agulhas Current meanders facilitate shelf-slope exchange on the eastern
1934 Agulhas Bank, J. Geophys. Res. Oceans, 123, 4762–4778,
1935 <https://doi.org/10.1029/2017JC013602>, 2018.

1936 Malauene, B. S., C. L. Moloney, C.L., Lett, C., Roberts, M. J., Marsac, F and Penven, P.: Impact
1937 of offshore eddies on shelf circulation and river plumes of the Sofala Bank, Mozambique
1938 Channel, J. Mar. Sys, 185, 1-12, 2018.

1939 Malauene, B. S., Lett, C., Marsac, F., Penven, P., Abdula, S., Moloney, C.L., Roberts, M.J.:
1940 Influence of Mozambique Channel eddies on larval loss of two shallow-water commercial
1941 shrimp species, 2024, Plos Climate, 3, e0000414, 2024.

1942 Maltrud, M. E., McClean, J. L.: An eddy resolving 1/10o Ocean Simulation. Ocean Model. 8,
1943 31-34, 2005.

1944 Marshall, T. A., Sigman, D. M., Beal, L. M., Foreman, A., Martínez-García, A., Blain, S., et al.:
1945 The Agulhas Current Transports Signals of Local and Remote Indian Ocean Nitrogen
1946 Cycling. J. Geophys Research: Oceans, 128(3). <https://doi.org/10.1029/2022JC019413>,
1947 2023.

1948 Mashifane, T.B., Braby, L., Pikiso, M., Sunnassee-Taukoor, S., Rapolaki, R.S., and Ragoasha,
1949 M.N.: Machine learning algorithm reveals surface deoxygenation in the Agulhas Current



1950 due to warming, *Prog. Oceanogr.*, 231, 103407,
1951 https://doi.org/10.1016/j.pocean.2024.103407, 2025.

1952 Mason, S.J.: Sea-surface temperature – South African rainfall associations, 1910–1989, *Int. J.*
1953 *Climatol.*, 15, 119–135, https://doi.org/10.1002/joc.3370150202, 1995.

1954 McGrath, A.M., Hermes, J.C., Moloney, C.L., Roy, C., Cambon, G., Herbette, S., and van der
1955 Lingen, C.D.: Investigating connectivity between two sardine stocks off South Africa using
1956 a high-resolution IBM: Retention and transport success of sardine eggs, *Fish. Oceanogr.*,
1957 29, 137–151, https://doi.org/10.1111/fog.12460, 2020.

1958 McMonigal, K., Beal, L.M., Elipot, S., Gunn, K.L., Hermes, J., Morris, T., and Houk, A.: The
1959 impact of meanders, deepening and broadening, and seasonality on Agulhas Current
1960 temperature variability, *J. Phys. Oceanogr.*, 50, 3529–3544, https://doi.org/10.1175/JPO-
1961 D-20-0018.1, 2020.

1962 Mordasova, N.V.: Chlorophyll in the southwestern Indian Ocean in relation to hydrologic
1963 conditions, *Oceanol.*, 20, 75–79, 1980.

1964 Morris, T., Scanderbeg M., West-Mack D., Gourcuff C., Poffa N., Bhaskar T.V.S.U., Hanstein
1965 C., Diggs S., Talley L., Turpin V., Liu Z. and Owens B.: Best practices for Core Argo
1966 floats - part 1: getting started and data considerations. *Front. Mar. Sci.* 11:1358042.
1967 https://doi.org/10.3389/fmars.2024.1358042, 2024

1968 Morris, T., D. Rudnick, J. Sprintall, J. Hermes, G. J. Goni, J. Parks, F. Bringas, E. Heslop, and
1969 the numerous contributors to the OCG-12 Boundary Current Workshop and OceanGliders
1970 BOON Project: Monitoring boundary currents using ocean observing infrastructure.
1971 *Frontiers in Ocean Observing: Documenting Ecosystems, Understanding Environmental*
1972 *Changes, Forecasting Hazards.* E.S. Kappel, S.K. Juniper, S. Seeyave, E. Smith, and M.
1973 Visbeck, eds, A Supplement to *Oceanography* 34(4),
1974 https://doi.org/10.5670/oceanog.2021.supplement.02-07, 2021

1975 Morris, T., Aguiar-González, B., Ansorge, I., & Hermes, J.: Lagrangian evolution of two
1976 Madagascar cyclonic eddies: Geometric properties, vertical structure, and fluxes. *Journal*
1977 *of Geophysical Research: Oceans*, 124, 8193–8218.
1978 https://doi.org/10.1029/2019JC015090, 2019

1979 Morris, T., Hermes, J., Beal, L., du Plessis, M., Duncombe Rae, C., Gulekana, M., Lamont, T.,
1980 Speich, S., Roberts, M., and Ansorge, I.J.: The importance of monitoring the Greater
1981 Agulhas Current and its inter-ocean exchanges using large mooring arrays, *S. Afr. J. Sci.*,
1982 113, #2016-0330, https://doi.org/10.17159/sajs.2017/20160330, 2017.

1983 Morris, T., Lamont, T., and Roberts, M.J.: Effects of deep-sea eddies on the northern KwaZulu-
1984 Natal shelf, South Africa, *Afr. J. Mar. Sci.*, 35, 343–350,
1985 https://doi.org/10.2989/1814232X.2013.827991, 2013.

1986 Nakamura, M.: Impacts of SST anomalies in the Agulhas Current System on the regional climate
1987 variability, *J. Climate*, 25, 1213–1229, https://doi.org/10.1175/JCLI-D-11-00088.1, 2012.

1988 Nehama, F. P. J. and Reason, C. J. C.: Modelling the Zambezi River plume, *African J. Marine*
1989 *Sci* 37, 593–604, 2015.

1990 New, A.L., Alderson, S.G., Smeed, D.A. and Stansfield, K.L.: On the Circulation of Water
1991 Masses across the Mascarene Plateau in the South Indian Ocean. *Deep Sea Resear Part I:*
1992 *Oceanographic Research Papers*, 54(1), 42–74, 2007.

1993 Nkwinkwa Njouodo, A.S., Koseki, S., Keenlyside, N., and Rouault, M.: Atmospheric signature
1994 of the Agulhas Current, *Geophys. Res. Lett.*, 45, 5185–5193,
1995 https://doi.org/10.1029/2018GL077042, 2018.

1996 Palastanga, V., van Leeuwen, P.J., and de Ruijter, W.P.M.: A link between low-frequency
1997 mesoscale eddy variability around Madagascar and the large-scale Indian Ocean
1998 variability, *J. Geophys. Res. Oceans*, 111, C09029,
1999 https://doi.org/10.1029/2005JC003081, 2006.



2000 Paula, J., Pinto, I., Guambe, I., Monteiro, S., Gove, D., and Guerreiro, J.: Seasonal cycle of
2001 planktonic communities at Inhaca Island, southern Mozambique, *J. Plankton Res.*, 20,
2002 2165–2178, <https://doi.org/10.1093/plankt/20.11.2165>, 1998.

2003 Penven, P., Backeberg, B., Braby, L., Halo, I., Hermes, J., Krug, M.: Revisiting Mesoscale
2004 Variability in the Agulhas System: A Decade Later, *Proceedings of the Nansen-Tutu*
2005 *Scientific Symposium*, 2025a.

2006 Penven, P., J.-F. Ternon, M. Noyon, S. Herbette, G. Cambon, C. Comby, P. L'Hégaret, B.
2007 S. Malauene, C. Ménesguen, F. Nehama, G. Rauntenbach, Y. Rufino, F. Sudre,
2008 Characterizing the central structure of a mesoscale eddy-ring dipole in the Mozambique
2009 Channel from in-situ observations, *J. Geophys. Res.*, 130, e2024JC021913, 2025b.

2010 Penven, P., Lutjeharms, J. R. E., Marchesiello, P., Roy, C., and Weeks, S. J.: Generation of
2011 cyclonic eddies by the Agulhas Current in the lee of the Agulhas Bank. *Geophys. Res.*
2012 *Lett.*, 27, 1055–1058, 2001.

2013 Penven, P., Lutjeharms, J.R.E., and Florenchie, P.: Madagascar: A pacemaker for the Agulhas
2014 Current system?, *Geophys. Res. Lett.*, 33, L17609,
2015 <https://doi.org/10.1029/2006GL026854>, 2006.

2016 Philips, H.E., Tandon, A., Furue, R., Hood, R., Ummenhofer, C.C., BenthuySEN, J.A., Menezes,
2017 V., Hu, S., Webber, B., Sanchez-Franks, A., Cherian, D., Shroyer, E., Feng, M.,
2018 Wijesekera, H., Chatterjee, A., Yu, L., Hermes, J., Murtugudde, R., Tozuka, T., Su, D.,
2019 Singh, A., Centurioni, L., Prakash, S., and Wiggert, J.: Progress in understanding of Indian
2020 Ocean circulation, variability, air-sea exchange, and impacts on biogeochemistry, *Ocean Sci.*, 17, 1677–1751, <https://doi.org/10.5194/os-17-1677-2021>, 2021.

2022 Porri, F., Jackson, J.M., von der Meden, C.E.O., Weidberg, N., and McQuaid, C.D.: The effect
2023 of mesoscale oceanographic features on the distribution of mussel larvae along the south
2024 coast of South Africa, *J. Mar. Syst.*, 132, 162–173,
2025 <https://doi.org/10.1016/j.jmarsys.2014.02.001>, 2014.

2026 Pringle, J., Stretch, D., and Tirok, K.: The geography of near-shelf mixing on the east coast of
2027 South Africa, *Environ. Fluid Mech.*, 23, 1145–1165, <https://doi.org/10.1007/s10652-022-09866-1>, 2023.

2029 Quartly, G.D., and Srokosz, M.A.: Eddies in the southern Mozambique Channel, *Deep-Sea Res.*
2030 II., 51, 69–83, <https://doi.org/10.1016/j.dsr2.2003.03.001>, 2004.

2031 Ramanantsoa, J.D., Penven, P., Krug, P., Gula, J., and Rouault, M.: Uncovering a New Current:
2032 The Southwest Madagascar Coastal Current, *Geophys. Res. Lett.*, 45, 1930–1938,
2033 <https://doi.org/10.1002/2017GL075900>, 2018.

2034 Ramanantsoa, J.D., Penven, P., Raj, R.P., Renault, L., Ponsoni, L., Ostrowski, M., Dilmahamod,
2035 A.F., and Rouault, M.: Where and how the East Madagascar Current Retroflection
2036 originates?, *J. Geophys. Res. Oceans*, 126, e2020JC016203,
2037 <https://doi.org/10.1029/2020JC016203>, 2021.

2038 Raw, J.L., van der Stocken, T., Carroll, D., Harris, L.R., Rajkaran, A., van Niekerk, L., and
2039 Adams, J.B.: Dispersal and coastal geomorphology limit potential for mangrove range
2040 expansion under climate change, *J. Ecol.*, 111, 139–155, <https://doi.org/10.1111/1365-2745.14020>, 2023.

2042 Reason, C.J.C.: Evidence for the influence of the Agulhas Current on regional atmospheric
2043 circulation patterns, *J. Climate*, 14, 2769–2778, [https://doi.org/10.1175/1520-0442\(2001\)014<2769:EFTIOT>2.0.CO;2](https://doi.org/10.1175/1520-0442(2001)014<2769:EFTIOT>2.0.CO;2), 2001.

2045 Renault, L., McWilliams, J. C., Penven, P.: Modulation of the Agulhas Current Retroflection
2046 and Leakage by oceanic current interaction with the atmosphere, *J. Phys. Oceanogr.*, 47,
2047 2077–2100, 2017.



2048 Richardson, P.L.: Agulhas leakage into the Atlantic estimated with subsurface floats and surface
2049 drifters, *Deep-Sea Res. I*, 54, 1361–1389, <https://doi.org/10.1016/j.dsr.2007.04.010>, 2007.
2050

2051 Ridderinkhof, H., and de Ruijter, W.P.M.: Moored current observations in the Mozambique
2052 Channel, *Deep-Sea Res. II*, 50, 1933–1955, [https://doi.org/10.1016/S0967-0645\(03\)00041-9](https://doi.org/10.1016/S0967-0645(03)00041-9), 2003.

2053 Roberts, M.J., Nieuwenhuys, C., and Guastella, L.A.: Circulation of the shelf waters in the
2054 KwaZulu-Natal Bight, South Africa, *Afr. J. Mar. Sci.*, 38, S7–S21,
2055 <https://doi.org/10.2989/1814232X.2016.1175383>, 2016.

2056 Rouault, M., Penven, P., and Pohl, B.: Warming in the Agulhas Current system since the 1980's.
2057 *Geophys. Res. Lett.*, 36, L12602, 2009.

2058 Rouault, M., Reason, C.J.C., Lutjeharms, J.R.E., and Beljaars, A.C.M.: Underestimation of
2059 latent and sensible fluxes above the Agulhas Current in NCEP and ECMWF analyses, *J.
2060 Climate*, 16, 776–782, [https://doi.org/10.1175/1520-0442\(2003\)016<0776:UOLASH>2.0.CO;2](https://doi.org/10.1175/1520-0442(2003)016<0776:UOLASH>2.0.CO;2), 2003.

2061 Roy, C., van der Lingen, C.D., Coetze, J.C., and Lutjeharms, J.R.E.: Abrupt environmental shift
2062 associated with changes in the distribution of Cape Anchovy *Engraulis encrasicolus*
2063 spawners in the southern Benguela, *Afr. J. Mar. Sci.*, 29, 309–319,
2064 <https://doi.org/10.2989/AJMS.2007.29.3.1.331>, 2007.

2065 Rühs, S., Schmidt, C., Schubert, R., Schulzki, T.G., Schwarzkopf, F.U., Le Bars, D., and
2066 Biastoch, A.: Robust estimates for the decadal evolution of Agulhas leakage from the
2067 1960s to 2010s, *Commun. Earth Environ.*, 3, 318, <https://doi.org/10.1038/s43247-022-00643-y>, 2022.

2068 Russo, C.S., Lamont, T., and Krug, M.: Spatial and temporal variability of the Agulhas
2069 Retroflection: Observations from a new objective detection method, *Remote Sens.
2070 Environ.*, 253, 112239, <https://doi.org/10.1016/j.rse.2020.112239>, 2021.

2071 Schmidt, C., Schwarzkopf, F.U., Rühs, S., and Biastoch, A.: Characteristics and robustness of
2072 Agulhas leakage estimates: an inter-comparison study of Lagrangian methods, *Ocean Sci.*,
2073 17, 1067–1080, <https://doi.org/10.5194/os-17-1067-2021>, 2021.

2074 Schouten, M. W., de Ruijter, W. P. M., and van Leeuwen, P. J.: Upstream control of Agulhas
2075 ring shedding., *J. Geophys. Res.*, 107, JC000804, 2002.

2076 Schouten, M.W., de Ruijter, W.P.M., van Leeuwen, P.J., and Ridderinkhof, H.: Eddies and
2077 variability in the Mozambique Channel, *Deep-Sea Res. II*, 50, 1987–2003,
2078 [https://doi.org/10.1016/S0967-0645\(03\)00042-0](https://doi.org/10.1016/S0967-0645(03)00042-0), 2003.

2079 Schubert R., Gula, J., Biastoch, A.: Submesoscale impacts on Agulhas leakage and Agulhas
2080 cyclone formation., *Nat. Comm. Earth Environ.*, 2, <https://doi.org/10.1038/s43247-021-00271-y>, 2021

2081 Schubert R., Schwarzkopf, F. U., Baschek, B., Biastoch, A.: Submesoscale impacts on
2082 mesoscale Agulhas dynamics, *J. Adv. Model. Earth Syst.*, 11, 2745–2767.
2083 <https://doi.org/10.1029/2019MS001724>, 2019.

2084 Schubert, R., Gula, J., Greatbatch, R. J., Baschek, B. and Biastoch, A.: The Submesoscale
2085 Kinetic Energy Cascade: Mesoscale Absorption of Submesoscale Mixed-Layer Eddies and
2086 Frontal Downscale Fluxes, *J. of Phys. Oceanogr.*, 50, 2573–2589, 2020.

2087 Schulzki, T., Schwarzkopf, F. U., and Biastoch, A.: Atlantic Meridional Overturning Response
2088 to Increased Southern Ocean Wind Stress in a Climate Model with an Eddy-Rich Ocean, *J.
2089 Clim*, 37, 5769–5792, <https://doi.org/10.1175/JCLI-D-23-0727.1>, 2024.

2090 Schumann, E.H., and Perrins, L.-A.: Tidal and intertidal currents around South Africa, *Coast.
2091 Eng. Proc.*, 1, 155, <https://doi.org/10.9753/icce.v18.155>, 1982.

2092

2093

2094

2095



2096 Schumann, E.H., Churchill, J.R.S., and Zaayman, H.J.: Oceanic variability in the western sector
2097 of Algoa Bay, South Africa, *Afr. J. Marine Sci.*, 27, 65–80,
2098 <https://doi.org/10.2989/18142320509504069>, 2005.

2099 Schumann, E.H., MacKay, C.F., and Strydom, N.A.: Nurdle drifters around South Africa as
2100 indicators of ocean structures and dispersion, *S. Afr. J. Sci.*, 115, #5372,
2101 <https://doi.org/10.17159/sajs.2019/5372>, 2019.

2102 Schwarzkopf, F.U., Biastoch, A., Böning, C.W., Chanut, J., Durgadoo, J.V., Getzlaff, K.,
2103 Harlaß, J., Rieck, J.K., Roth, C., Scheinert, M.M., and Schubert, R.: The INALT family –
2104 a set of high-resolution nests for the Agulhas Current system within global NEMO
2105 ocean/sea-ice configurations, *Geosci. Model Dev.*, 12, 3329–3355,
2106 <https://doi.org/10.5194/gmd-12-3329-2019>, 2019.

2107 Shchepetkin, A.F., and McWilliams, J.C.: The regional oceanic modelling system (ROMS): a
2108 split-explicit, free-surface, topography-following-coordinate oceanic model, *Ocean
2109 Model.*, 9, 347–404, <https://doi.org/10.1016/j.ocemod.2004.08.002>, 2005.

2110 Sieler, G., Rouault, M., and Lutjeharms, J.R.E.: Structure and origin of the subtropical South
2111 Indian Ocean Countercurrent, *Geophys. Res. Lett.*, 33, L24609,
2112 <https://doi.org/10.1029/2006GL027399>, 2006.

2113 Sieler, G., Rouault, M., Biastoch, A., Backeberg, B., Reason, C.J.C., and Lutjeharms, J.R.E.:
2114 Modes of the southern extension of the East Madagascar Current, *J. Geophys. Res. Oceans*,
2115 114, C01005, <https://doi.org/10.1029/2008JC004921>, 2009.

2116 Silva, C.N.S., Young, E.F., Murphy, N.P., Bell, J.J., Green, B.S., Morley, S.A., Duhamel, G.,
2117 Cockcroft, A.C., and Strugnell, J.M.: Climatic change drives dynamic source-sink
2118 relationships in marine species with high dispersal potential, *Ecol. Evol.*, 11, 2535–2550,
2119 <https://doi.org/10.1002/ece3.7204>, 2021.

2120 Singleton, A.T., and Reason, C.J.C.: A numerical model study of an intense cutoff low pressure
2121 system over South Africa, *Mon. Weather Rev.*, 135, 1128–1150,
2122 <https://doi.org/10.1175/MWR3311.1>, 2007.

2123 Singleton, A.T., and Reason, C.J.C.: Numerical simulations of a severe rainfall event over the
2124 Eastern Cape coast of South Africa: sensitivity to sea surface temperature and topography,
2125 *Tellus A: Dyn. Meteorol. Oceanogr.*, 58, 335–367, <https://doi.org/10.1111/j.1600-0870.2006.00180.x>, 2006.

2127 Sinyanya, K. Y., Marshall, T. A., Flynn, R. F., Harris, E., Mdutyana, M., Roman, R., et al.:
2128 Wintertime productivity and Carbon export potential across the Agulhas Current system.
2129 Deep-Sea Res Part I: Oceanographic Research Papers, 213.
2130 <https://doi.org/10.1016/j.dsr.2024.104405>, 2024.

2131 Speich, S., Lutjeharms, J. R. E., Penven, P., and Blanke, B.: Role of bathymetry in agulhas
2132 current configuration and behaviour. *Geophys. Res. Lett.*, 33, L23611, 2006.

2133 Sudre, F., Dewitte, B., Mazoyer, C., Garçon, V., Sudre, J., Penven, P., Rossi, V.: Spatial and
2134 seasonal variability of horizontal temperature fronts in the Mozambique Channel for both
2135 epipelagic and mesopelagic realms, *Front. Mar. Sci.*, 9, 1045136, 2023.

2136 Tew-Kai, E., and Marsac, F.: Patterns of variability of sea surface chlorophyll in the
2137 Mozambique Channel: A quantitative approach, *J. Mar. Syst.*, 77, 77–88,
2138 <https://doi.org/10.1016/j.jmarsys.2008.11.007>, 2009.

2139 Thoppil, P. G., Richman, J. G., Hogan P. J. et al.: Energetics of a global ocean circulation model
2140 compared to observations, *Geophys. Res. Lett.*, 38, L15607, doi:10.1029/2011GL048347,
2141 20

2142 van der Lingen, C.D., Hutchings, L., Lamont, T., and Pitcher, G.C.: Climate change,
2143 dinoflagellate blooms and sardine in the southern Benguela Current Large Marine
2144 Ecosystem, *Environ. Dev.*, 17, 230–243, <http://doi.org/10.1016/j.envdev.2015.09.004>,
2145 2016.



2146 van Leeuwen, P. J., de Ruijter, W. P. M., and Lutjeharms, J. R. E.: Natal Pulses and the formation
2147 of Agulhas rings. *J. Geophys. Res.*, 105, 6425–6436, 2000.

2148 van Sebille, E., Barron, C.N., Biastoch, A., van Leeuwen, P.J., Vossepoel, F.C., and de Ruijter,
2149 W.P.M.: Relating Agulhas leakage to the Agulhas Current retroflection location, *Ocean
2150 Sci.*, 5, 511–521, <https://doi.org/10.5194/os-5-511-2009>, 2009a.

2151 van Sebille, E., Beal, L.M., and Biastoch, A.: Sea surface slope as a proxy for Agulhas current
2152 strength, *Geophys. Res. Lett.*, 37, L09610, <https://doi.org/10.1029/2010GL042847>, 2010.

2153 van Sebille, E., Biastoch, A., van Leeuwen, P.J., and de Ruijter, W.P.M.: A weaker Agulhas
2154 Current leads to more Agulhas leakage, *Geophys. Res. Lett.*, 36, L03601,
2155 <https://doi.org/10.1029/2008GL036614>, 2009b.

2156 Villar, E., Farrant, G.K., Follows, M., Garczarek, L., Speich, S., Audic, S., Bittner, L., Blanke,
2157 B., Brum, J.R., Brunet, C., Casotti, R., Chase, A., Dolan, J.R., d'Ortenzio, F., Gattuso, J.-
2158 P., Grimá, N., Guidi, L., Hill, C.N., Jahn, O., Jamet, J.-L., Le Goff, H., Lepoivre, C.,
2159 Malviya, S., Pelletier, E., Romagnan, J.-B., Roux, S., Santini, S., Scalco, E., Scwenck,
2160 S.M., Tanaka, A., Testor, P., Vannier, T., Vincent, F., Zingone, A., Dimier, C., Picheral,
2161 M., Searson, S., Kandels-Lewis, S., Tara Oceans Coordinators, Acinas, S.G., Bork, P.,
2162 Boss, E., de Vargas, C., Gorsky, G., Ogata, H., Pesant, S., Sullivan, M.B., Sunagawa, S.,
2163 Wincker, P., Karsenti, E., Bowler, C., Not, F., Hingamp, P., and Iudicone, D.:
2164 Environmental characteristics of Agulhas rings affect interocean plankton transport,
2165 *Science*, 348, 1261447, <https://doi.org/10.1126/science.1261447>, 2015.

2166 Walker, N.D.: Links between South African summer rainfall and temperature variability of the
2167 Agulhas and Benguela Current Systems, *J. Geophys. Res. Oceans*, 95, 3297–3319,
2168 <https://doi.org/10.1029/JC095iC03p03297>, 1990.

2169 Weijer, W., de Ruijter, W.P.M., Sterl, A., and Drijfhout, S.S.: Response of the Atlantic
2170 overturning circulation to South Atlantic sources of buoyancy, *Global Planet. Change*, 34,
2171 293–311, [https://doi.org/10.1016/S0921-8181\(02\)00121-2](https://doi.org/10.1016/S0921-8181(02)00121-2), 2002.

2172 Weijer, W. and van Sebille, E.: Impact of Agulhas Leakage on the Atlantic Overturning
2173 Circulation in the CCSM4, *J. Clim.*, 27, 101–110, [https://doi.org/10.1175/JCLI-D-12-00714.1](https://doi.org/10.1175/JCLI-D-12-
2174 00714.1), 2014.

2175 Wells, C., Pringle, J., and Stretch, D.D.: Cold water pathways and regional flow patterns in the
2176 southwest Indian Ocean associated with temperature anomalies on the Sodwana reef
2177 system, *South Africa, Estuar. Coast. Shelf Sci.*, 287, 108337,
2178 <https://doi.org/10.1016/j.ecss.2023.108337>, 2023.

2179 Wells, C., Pringle, J., and Stretch, D.D.: Cold water temperature anomalies on the Sodwana reefs
2180 and their driving mechanisms, *S. Afr. J. Sci.*, 117, #9304,
2181 <https://doi.org/10.17159/sajs.2021/9304>, 2021.

2182 Wells, C., Pringle, J., and Stretch, D.D.: Refining the role of bathymetry, hydrodynamics and
2183 upwelling at various scales along the coral reefs at Sodwana Bay, South Africa, *Ocean
2184 Dynam.*, 75, 13, <https://doi.org/10.1007/s10236-024-01646-3>, 2025.

2185 Wells, C., Pringle, J., and Stretch, D.D.: Upwelling along the southeast African coastline and
2186 links to cold water temperature anomalies at Sodwana Bay, South Africa, *Cont. Shelf Res.*,
2187 276, 105227, <https://doi.org/10.1016/j.csr.2024.105227>, 2024.

2188 Zhu, Y., Qiu, B., Lin, X., Wang, F.: Interannual eddy kinetic energy modulations in the Agulhas
2189 Return Current, *J. Geophys. Res.*, 123, <https://doi.org/10.1029/2018JC014333>, 2018